

LEGIBILITY NOTICE

A major purpose of the Technical Information Center is to provide the broadest dissemination possible of information contained in DOE's Research and Development Reports to business, industry, the academic community, and federal, state and local governments.

Although a small portion of this report is not reproducible, it is being made available to expedite the availability of information on the research discussed herein.

LA-UR- 87 - 27 47

1987

CONF-8705193--1

Los Alamos National Laboratory is operated by the University of California for the United States Department of Energy under contract W-7405-ENG-36

TITLE: DIMENSIONAL ANALYSIS OF HEART RATE VARIABILITY IN HEART TRANSPLANT RECIPIENTS*)

LA-UR--87-2747

AUTHOR(S): Gottfried Mayer-Kress
John P. Zbilut
Karlheinz Geist

DE87 014773

SUBMITTED TO: Proceedings for the 7th Annual CNLS Workshop "Nonlinearity in Biology and Medicine".

DISCLAIMER

This report was prepared as an account of work sponsored by an agency of the United States Government. Neither the United States Government nor any agency thereof, nor any of their employees, makes any warranty, express or implied, or assumes any legal liability or responsibility for the accuracy, completeness, or usefulness of any information, apparatus, product, or process disclosed, or represents that its use would not infringe privately owned rights. Reference herein to any specific commercial product, process, or service by trade name, trademark, manufacturer, or otherwise does not necessarily constitute or imply its endorsement, recommendation, or favoring by the United States Government or any agency thereof. The views and opinions of authors expressed herein do not necessarily state or reflect those of the United States Government or any agency thereof.

By acceptance of this article, the publisher recognizes that the U.S. Government retains a nonexclusive, royalty-free license to publish or reproduce the published form of this contribution, or to allow others to do so, for U.S. Government purposes.

The Los Alamos National Laboratory requests that the publisher identify this article as work performed under the auspices of the U.S. Department of Energy.

MASTER

Los Alamos Los Alamos National Laboratory
Los Alamos, New Mexico 87545

DISTRIBUTION OF THIS DOCUMENT IS UNLIMITED



**Dimensional Analysis of Heart Rate Variability in Heart
Transplant Recipients*)**

**John P. Zbilut
Graduate College of Nursing
Rush University, Chicago, IL 60612**

**Gottfried Mayer-Kress
Laboratory for Biological Dynamics and Theoretical Medicine
and Institute for Nonlinear Science, UCSD
Crump Institute for Medical Engineering, UCLA
Center for Nonlinear Studies, MS-B258, LANL, Los Alamos, NM 87545**

**Karlheinz Geist
Center for Nonlinear Studies, MS-B258, LANL, Los Alamos, NM 87545
3. Phys. Inst., Univ. Göttingen, W.-Germany**

Abstract

Periodicities in the heart rate have been known for some time. We discuss these periodicities in normal and transplanted hearts. We then consider the possibility of dimensional analysis of these periodicities in transplanted hearts and problems associated with the record.

*) Running Title: Dimensional Analysis of Transplanted Hearts

1. Introduction to Heart Rate Periodicities.

The spontaneous beat-to-beat variability of the heart record has been known for some time to have approximate periodicities. Researchers have identified three bands of spectral activity in adults: low frequency (approximately 0.05 Hz) related to thermoregulation; a slightly higher frequency (approximately 0.1 Hz) associated with baroreceptor feed-back control; and a region between 0.12 – 0.5 Hz corresponding to the respiratory frequency [1,2] (Fig. 1). These periodicities are not constant, and often fluctuate, disappear, and may be entrained to each other as may be the case with the respiratory periodicity as it approaches the baroreceptor frequency[3]. Research has shown that all of these periodicities are modulated to various degrees by the autonomic nervous system and humoral agents such as renin-angiotensin[4].

The beat-to-beat interval is typically derived from the depolarization voltage of the ventricles identified on the normal electrocardiogram as the *QRS* complex. Although technically the origination of the heart beat occurs at the sinus node with the beginning of the P wave, the *QRS* complex with its R wave potential is greater, and typically the signal-to-noise ratio is considerably better. Using the R wave with a suitable level detector can allow for timing accuracy in the range of 0.1 msec. It is necessary, however, to remember that by using the R wave to estimate intervals, bias and variance do exist[5]. The bias is due to intermediary conduction times between the sinus node and His bundle which is approximately 60 msec, and may fluctuate up to 10 msec on a beat-to-beat basis. This is usually of no problem unless specific physiologic processes are being correlated. Variance can be a problem with decreasing interval fluctuations.

2. Interval Variability and the Transplanted Heart.

The usual method of heart transplantation results in extrinsic denervation[6]. Although the old sinus node remains in the atrial remnant of the recipient, to date there has been no evidence that the signal of the old sinus node crosses the suture line to the new heart. Instead, the beat-to-beat depolarization of the transplanted heart is governed by the new heart's sinus node[7]. Thus, the usual neural feedback mechanisms responsible for governance of the heart rate are no longer present, except perhaps for some afferent receptors in the atrial remnant[8]. Instead, intracardiac and humoral mechanisms modulate heart rate variability. As a consequence, the resting heart rate is higher (e.g. 90-100 beats/min.). Regulation of heart-beat in response to physical demands such as exercise is still present, although at a slower response time through circulating agents such as adrenaline[9]. Heart rate periodicities are also present in the denervated heart, but of a greatly attenuated amplitude[10].

A constant concern regarding the transplanted heart is that of tissue rejection, which is monitored periodically by intra-cardiac biopsy. Inspection of the power spectrum of the intervals has revealed a statistically significant decrease in the peak spectral peak of the respiratory band, approaching broad band noise[11](Figs. 2-5).

3. Rational for Dimensional Analysis of Heart Beat Intervals in Transplanted Hearts

The term dimension has been used to refer to the number of independent vectors necessary to specify the state of a dynamical system. Dimensional analysis of the heart beat intervals, therefore, suggests an analysis of the variables regulating its beating.

Previously, simple phase plane analyses of intervals produced by Soviet researchers were noted to be striking in that orbits were severely compressed or expanded in subjects during various phases of sleep, and with cardiac pathology[12]. However, it has also been noted that physiologic parameters may be difficult to analyze dimensionally due to lack of stationarity of the system[13]. As a result, transplanted hearts were selected for analysis with the hypothesis that denervation would reduce the number of dimensions necessary to model them.

A major problem with interval analysis is the acquisition of sufficient data points while maintaining relative stationarity. For example to obtain 1000 data points from an individual whose heart is beating 100 *beats/min* requires a subject to remain relatively stimulus free for 10 *minutes*. And although environmental stimuli can be controlled, psychological processes cannot, and may affect the heart rate. As a result, we proceeded with relatively short data sets as an initial exploration. Some support for such an approach has been produced, but needs to be further substantiated[14]. We plan to improve the statistical accuracy of the results by implementing a reconstruction method which uses non-contiguous data-segments (see e.g. [22,24]).

4. Dimensional Analysis of Heart Transplant Intervals.

We chose several subjects with a view toward sampling in the immediate post-transplant period, during normal functioning, and during periods of rejection.

To calculate the "dimension" of intervals, it is necessary first to reconstruct the attractor from the time-series [24]. This is done by creating vectors \vec{x}_m in an n -dimensional state-space by taking beat-delayed samples (with a delay k determined from the first minimum of the mutual information content [16,23]) of the interval data x_m . This is to say that phase portraits of dimension n are constructed such that: $\vec{x}_m = (x_m, x_{m-k}, x_{m-2k}, \dots, x_{m-(n-1)k})$ where m runs from 1 to the number n_{data} of data points[15,16].

Phase portraits ($n = 2$) reveal chaotic orbits in both rejecting and non-rejecting hearts. There seem to be two regions of heart rates present which could be interpreted as two different attractors and the patient undergoes a transition from to the other. In Figs. 6-9 we have the timeseries of heart rates as well as their phase portraits for two different delays.

We have implemented several different and largely independent algorithms for the dimension calculation. The Grassberger and Procaccia method of dimension calculation [17,18] yields a very coarse averaged quantity with a very large and difficult to estimate error[18].

In standard use currently, the method determines the correlation integral $C(r)$, which is obtained by averaging over the number $N_{\vec{x}_m}(r)$ of data vectors \vec{x}_i contained in a neighborhood of size r of a reference vector \vec{x}_m :

$$N_{\vec{x}_m}(r) = \sum_{i=1}^{n_{data}} \Theta(r - \|\vec{x}_i - \vec{x}_m\|) \quad (1)$$

where Θ is the Heavyside function. The averaging is done over a characteristic set of n_{ref} reference points \vec{x}_m , i.e.

$$C(r) = \lim_{n_{data} \rightarrow \infty} \frac{1}{n_{ref}} \sum_{m=1}^{n_{ref}} \frac{1}{n_{data}} N_{\vec{x}_m}(r) \quad (2)$$

where Θ is the Heavyside function. The averaging is done over a characteristic set of n_{ref} reference points \vec{x}_m , i.e.

$$C(r) = \lim_{n_{data} \rightarrow \infty} \frac{1}{n_{ref}} \sum_{m=1}^{n_{ref}} \frac{1}{n_{data}} N_{\vec{x}_m}(r) = \lim_{n_{data} \rightarrow \infty} \frac{1}{n_{data}} \langle N_{\vec{x}_m}(r) \rangle_{\vec{x}_m} \quad (3)$$

In a log-log-representation this function typically exhibits a scaling region

over which a slope can be defined which is then interpreted as the Grassberger Procaccia dimension of the system (see e.g. [17,18,22,23]). The errors of this method represent the statistical spread of $N_{\vec{x}_m}(r)$ which depends to a large extent on the degree of non-uniformity of the dynamics producing the time series. In table 1 we therefore only give our estimates of the Grassberger Procaccia dimension without errors. In the estimate we used a delay of 4 beats and fitted over a range $\log_2(\frac{r_{max}}{r_{min}}) = 0.5$

Because of this very unsatisfactory effect we modified our approach in a way that we compute for the "gauge-function" $N_{\vec{x}_m}(r)$ the pointwise dimension $d_{\vec{x}_m}$ at each of the reference points separately (with the same delay and fit range) and then average over the obtained n_{ref} dimension values (for more details see [23]).

In this way we are able to take better care of the variation of the local properties of the attractor. In order to demonstrate this method we have chosen one case (1611) as an example for the different ways we have to analyze the datafile: In Fig. 10 we have for a given reference point \vec{x}_m and embedding dimensions $n = 1, \dots, 20$ the local gauge function $N_{\vec{x}_m}(r)$. For a comparison we have applied a method recently introduced by Broomhead and King [26], which is based on singular value decomposition. Here the datavectors \vec{x}_m are transformed into a basis in which the representation appears to be more uniform and therefore the results look more stable (there are several caveats in place for the application of this method which will be discussed elsewhere [29]).

In both methods we made sure that the reconstructed vectors covered approximately, the same number of beats (i.e. with maximal embedding dimension 20 and delay $k = 4$ we cover 80 beats in the case of the Grassberger-Procaccia case and in the case of singular value decomposition we have chosen a window of 100 beats). In Fig. 11 we have the same local gauge function as in Fig. 10 but after the transformation into the new basis. In Fig. 12 we have the computed pointwise dimension as a function of the number of the reference point. The points without errorbars indicate a goodness of fit (GF) which is better than 0.2. In Fig. 13 we see the effect of the singular value decomposition (SV), now all reference points have a $GF < 0.2$. In Fig. 14 we plot a histogram of pointwise dimension values

without (solid line) and with (broken line) SV for an embedding dimension of $n = 20$. In Fig. 15 we see how the estimated dimension value depends on the embedding dimension both for the case of SV (broken line) and without (solid line). Note the fast saturation for SV which is due to the fact that only a few singular values are significantly different from zero. In Fig. 16 we plot the fraction of the number of reference points which reach a certain GF as a function of GF and the embedding dimension. We see that only at about $GF = 0.4$ all of the reference points allow the estimation of a pointwise dimension with the above criteria. This changes radically with the SV where already for a goodness of fit of $GF = 0.1$ basically all the reference points are accepted. In Fig. 17 we see the dependence of the estimated dimension ($D_{A.P.}$) on the GF and the embedding dimension and in Fig. 18 we have the same plot for $D_{S.V.}$. In Figs. 19-20 we show the corresponding standard deviations, and again it is clear that the results appear much more noise-free after SV. In Fig. 21 we show how the histogram of $D_{A.P.}$ (see Fig. 14) depends on the embedding dimension and in Fig. 22 we have the same plot for $D_{S.V.}$. Note how in Fig. 21 a double peaked distribution evolves. It appears that this double peak distribution of $D_{A.P.}$ is most evident for small values of GF (Fig. 23).

5. Summary of Calculations for the Heart Beat Intervals.

Table 1 summarizes the Grassberger-Procaccia dimensions and the averaged pointwise dimension with and without singular value decomposition for the heart rate data. It will be noted that there is relatively poor fit for the untransformed data without singular value decomposition (SV). This suggests poor resolution in scaling regions and may be possibly a result of two related mechanisms: 1) the decreased amplitude of periodicities in the denervated heart; and 2) the use of the R wave instead of the P wave to detect the beat in such diminished fluctuations. Nonetheless, comparing these two data sets insofar as they are similar in data points and fits, it would appear that rejection (1611) is heralded by a decrease in dimensionality (except for $D_{G.P.}$) (Figs. 15, 24-26). In the two hearts without rejection the dimensionality seems to be increased with the exception of $D_{S.V.}$ of case 1726. In view of the small differences and the large error bars for only very few cases it is clear that much more work needs to be done before statistically significant statements can be made.

It is tempting to conjecture that the hypothesis put forth by Goldberger et al.; namely, that disease states are characterized by paradoxical order, is operative here in terms of reduction of dimensions[20]. Indeed the suggestion of J. Doyno Farmer that death may be the ultimate fixed point may have profound implications for the study of physiologic processes[21].

Certainly, a greater number of data points, or more data with multiple subjects could help clarify the situation. For example, if the true dimensionality of a non-rejecting heart is approximately 5, then at least 10^5 data points would be required[22]. This would entail perhaps 24 hrs of stationary recording. The implication here, is that subjects and conditions must be carefully chosen, since it appears that the heart beat interval may not easily be described by a low dimensional attractor.

Table 1:

TYPE OF HEART	$D_{G.P.}$	$D_{A.P.}$	$D_{S.V.}$
2 WEEKS POST			
TRANSPLANT (1271)	5.3	5.9 ± 1.8	3.2 ± 1.4
REJECTING (1611)	7.3	3.1 ± 1.9	2.9 ± 0.9
NON-REJECTING(8212)	6.1	5.9 ± 2.7	3.6 ± 1.8
NON-REJECTING(1726)	6.5	3.5 ± 1.6	2.6 ± 1.0

6. Conclusions.

1. The beat-to-beat intervals of transplant recipients appear to be modeled by high dimensionality, and are relatively non-stationary. This occurs despite well-controlled physical circumstances. Psychological processes may be responsible.

2. There appears to be a reduction of dimensionality with rejection, suggesting a possible inability to react to multiple feed-back control systems. This may be a part of a larger process characteristic of pathology whereby dimensionality decreases as a result of transitions away from deterministic chaos, or collapse upon a lower dimensional orbit.

3. Confirmation of the above requires longer data sets with possibly better resolution of intervals derived from P wave detection.

4. Until such confirmation is obtained, it is probably better to speak of apparent dimension or dimensionality, instead of dimension in the strict sense.

7. Acknowledgement.

We thank D. Murdock, L. Lawson, D. Farmer and J. Sidorowich for helpful discussions. This work was supported by a National Research Service Award from NIH, NCNR, NU 05867-01.

References

1. *Book* R. I. Kitney, O. Rompelman, *The Study of Heart-Rate Variability* (Oxford Univ. Press, Oxford, 1980).
2. *Journal* B. McA. Sayers, *Ergonomics* 16, 17 (1973).
3. *Journal* D. P. Giddens, R. I. Kitney, *J. Theor. Biol.* 113, 759 (1985).
4. *Journal* S. Akselrod, D. Gordon, F. A. Ubel, D. C. Shannon, A. C. Barger, R. J. Cohen, *Science* 213, 220 (1981).
5. *Book* O. Rompelman, *Cardiorespiratory and Cardiosomatic Psychophysiology*, ed. by P. Grossman, K. H. L. Janssen, D. Vaitl (Plenum Press, New York, 1986), p. 65.
6. *Journal* R. R. Lower, N. E. Shumway, *Surg. Forum* 11, 18 (1960).
7. *Journal* J. W. Mason, E. B. Stinson, D. C. Harrison, *Cardiology* 61, 75 (1976).
8. *Journal* R. R. Lower, *Am. Heart J.* 71, 841 (1966).
9. *Journal* H. K. Hammond, V. F. Froelicher, *Prog. Cardiovasc. Dis.* 27, 271 (1985).
10. *Journal* J. Zbilut, D. Murdock, C. Lawless, L. Lawson, M. Von Dreele, S. Porges, *Clin. Res.* 34, 906A (1986).
11. *Edited Book* J. Zbilut, D. Murdock, L. Lawson, C. Lawless, M. Von Dreele, S. Porges: submitted to *60th Scientific Sessions of the American Heart Association*
12. *Edited Book* D. Zhemajyte, L. Tel'ksnys (eds.), *Analiz Serdechnogo Ritma [Analysis of the Heart Rhythm]*, (Mokslac, Vilnius, 1982).
13. *Edited Book* S. P. Layne, G. Mayer-Kress, J. Holzfuss in *Dimensions and Entropies in Chaotic Systems*, ed. by G. Mayer-Kress (Springer, Heidelberg, 1986).
14. *Journal* J. Kurths, H. Herzog, *Physica* 25D, 165 (1987).
15. *Journal* N. H. Packard, J. P. Crutchfield, J. D. Farmer, R. S. Shaw, *Phys. Rev. Lett.* 45, 712 (1980).
16. *Edited Book* A. M. Fraser in *Dimensions and Entropies in Chaotic Systems*, ed. by G. Mayer-Kress (Springer, Heidelberg, 1986).
17. *Journal* P. Grassberger, I. Procaccia: *Phys. Rev. Lett.* 50, 346 (1983).
18. *Edited Book* J. Holzfuss, G. Mayer-Kress in *Dimensions and Entropies in Chaotic Systems*, ed. by G. Mayer-Kress (Springer, Heidelberg, 1986).
19. *Journal* D. K. Murdock, C. E. Lawless, H. S. Loeb, P. J. Scanlon, R. Pifarr, *J. Heart Transplant.* 5, 336 (1986).
20. *Journal* A. L. Goldberger, L. J. Findley, M. R. Blackburn, A. J. Mandell, *Am. Heart J.* 107, 612 (1984).
21. *Private communication* 21. J. Doyne Farmer: private communication.
22. *Journal* G. Mayer-Kress, F. Eugene Yates, Laurel Benton, M. Keidel, W. Tirsch, S.J. Poepl, K. Geist, *Nonlinear Oscillations in Brain, Heart and Muscle*, this volume
23. *Edited Book* G. Mayer-Kress: Los Alamos Preprint LA-UR-87-1030, and to appear in *Directions in Chaos*, Hao Bai-Lin (ed.), World Scientific.
24. *Journal* N. H. Packard, J. P. Crutchfield, J. D. Farmer, R. S. Shaw, "Geometry From a Time Series", *Phys. Rev. Lett.* 45, 712, 1980
25. *Edited Book* F. Takens *Detecting Strange Attractors in Turbulence*, in *Lecture Notes in Mathematics* 898, D. A. Rand L. S. Young (eds.), Springer, Berlin 1981

26. *Journal* D. S. Broomhead, G.P. King *Extracting qualitative dynamics from experimental data*, *Physica D*, 1986
27. *Journal* J. D. Farmer, E. Ott, J. A. Yorke, *The Dimension of Chaotic Attractors*, *Physica D*, 153 (1983)
28. *Journal* J. Ramsey, *The Statistical Properties of Dimension Calculations using Small Data Sets*, Preprint 1987

Figure Captions

- Fig. 1: Log power spectrum of normal adult heart beat intervals. Three regions of activity are seen: 1) near 0.05; 2) near 0.1; and 3) near 0.3. (For this and subsequent plots, the Welch method of spectral analysis, incorporating a Hanning window, was used for a data set of 1024 intervals and averaged over segments of 256 to reduce variance. Frequencies are in Hertz equivalents; spectral units are $\log_{10}/msec^2/cycle/beat$.)
- Fig. 2: Log power spectrum of a denervated heart 2 weeks post-transplant, and subject to Cheyne-Stokes respirations (1271).
- Fig. 3: Log power spectrum of a heart experiencing rejection (1611).
- Fig. 4: Log power spectrum of a non-rejecting heart (8212).
- Fig. 5: Log power spectrum of a non-rejecting heart from a different subject (1726).
- Fig. 6: Timeseries of heart rates of denervated heart (1271) and phase portrait for delays $\tau = 1$ and $\tau = 4$.
- Fig. 7: Same as Fig. 6 for rejecting heart (1611).
- Fig. 8: Same as Fig. 6 for non-rejecting heart (8212).
- Fig. 9: Same as Fig. 6 for non-rejecting heart (1726).
- Fig. 10: Local gauge function for embedding dimensions $n = 1, \dots, 20$ for rejecting heart (1611). The solid lines indicate fits with a goodness of fit (GF) of 0.2. The broken lines indicate a fit for which $GF > 0.2$. The size of the errorbar is a measure for GF relative to $GF = 0.2$.
- Fig. 11: Same as in Fig. 10 after singular value decomposition (SV).
- Fig. 12: Pointwise dimension as a function of the number of the reference point for case 1611. Points without errorbars indicate $GF < 0.2$ (case 1611).
- Fig. 13: Same as in Fig. 12 after singular value decomposition.
- Fig. 14: Histogram of pointwise dimension values without ($D_{A.P.}$) (solid line); and with (broken line) SV ($D_{S.V.}$) for an embedding dimension of $n = 20$ (case 1611).
- Fig. 15: Estimated dimension without SV ($D_{A.P.}$) (solid errorbars) and with SV ($D_{S.V.}$) (broken errorbars) as a function of the embedding dimension n . The errorbars correspond to the standard deviation taken over all reference points (case 1611).
- Fig. 16: Fraction of the number of reference points which reach a certain GF as a function of GF and the embedding dimension (case 1611).
- Fig. 17: Dependence of the estimated dimension ($D_{A.P.}$) on the GF and the embedding dimension (case 1611).
- Fig. 18: Same as in Fig. 17 for $D_{S.V.}$.
- Fig. 19: Standard deviation of the dimension values of Fig. 17
- Fig. 20: Standard deviation of the dimension values of Fig. 18

Fig. 21: Histogram of pointwise dimension values $D_{A.P.}$ as a function of the embedding dimension ($GF = 0.2$). The dotted line at $P = 0$ denotes the average of the distribution.

Fig. 22: Same as in Fig. 21 for $D_{S.V.}$

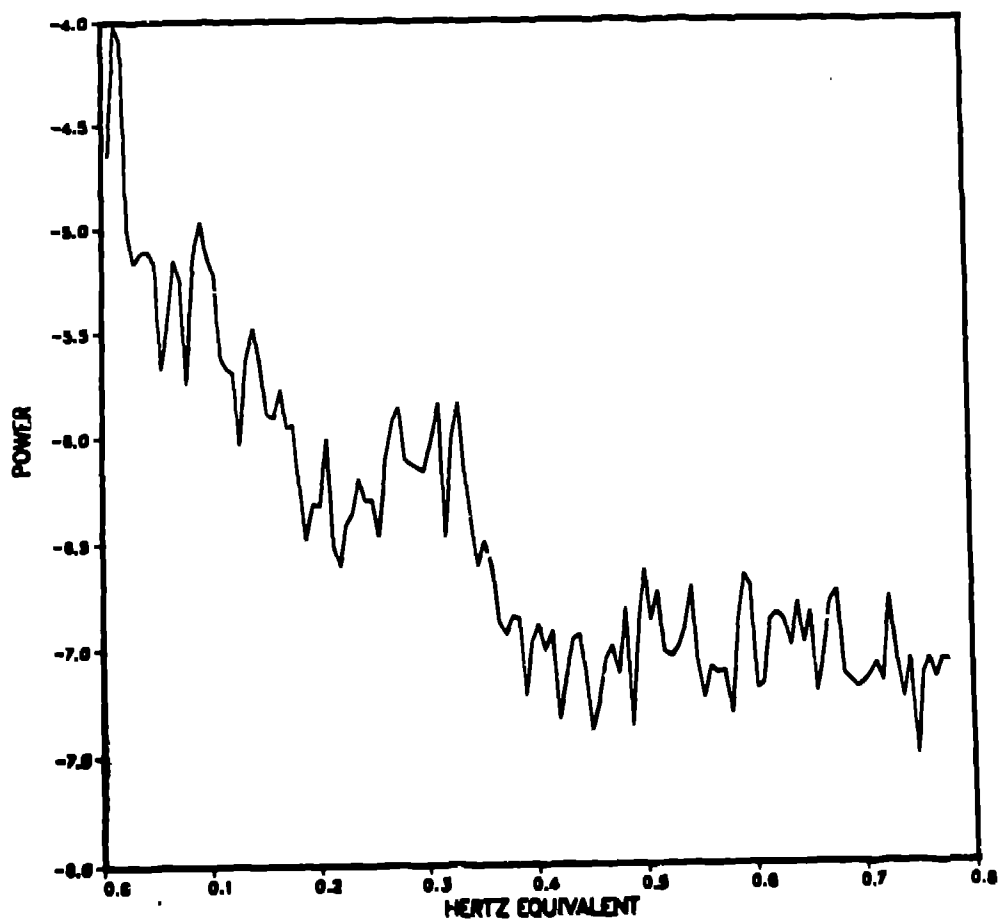
Fig. 23: Histogram of pointwise dimension values $D_{A.P.}$ as a function of the goodness of fit (GF).

Fig. 24: Same as Fig. 15 for case 1271

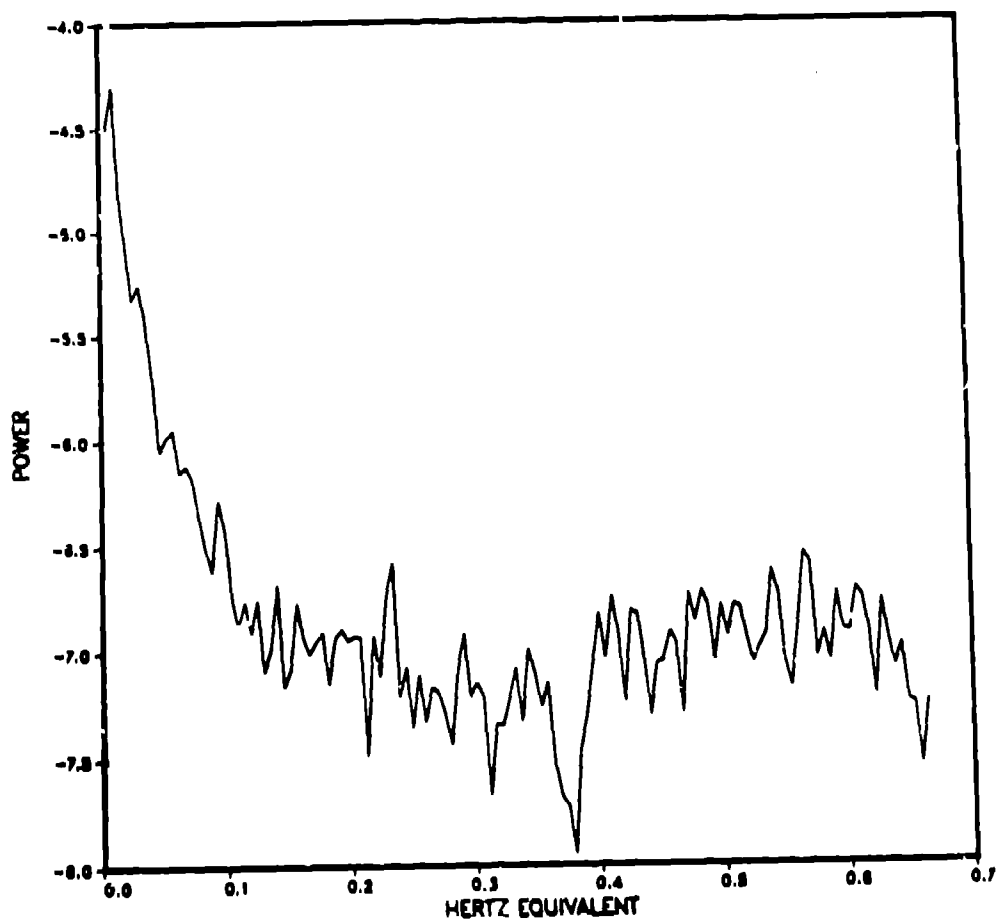
Fig. 25: Same as Fig. 15 for case 8212

Fig. 26: Same as Fig. 15 for case 1726

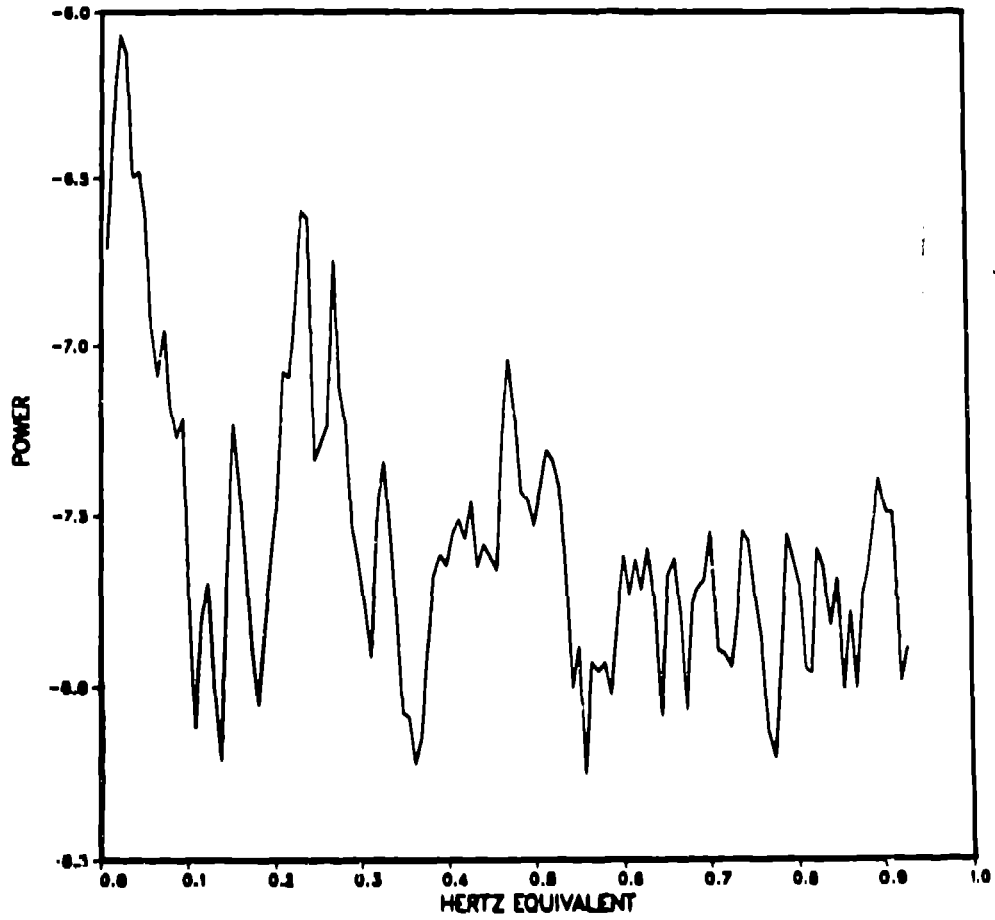
norma



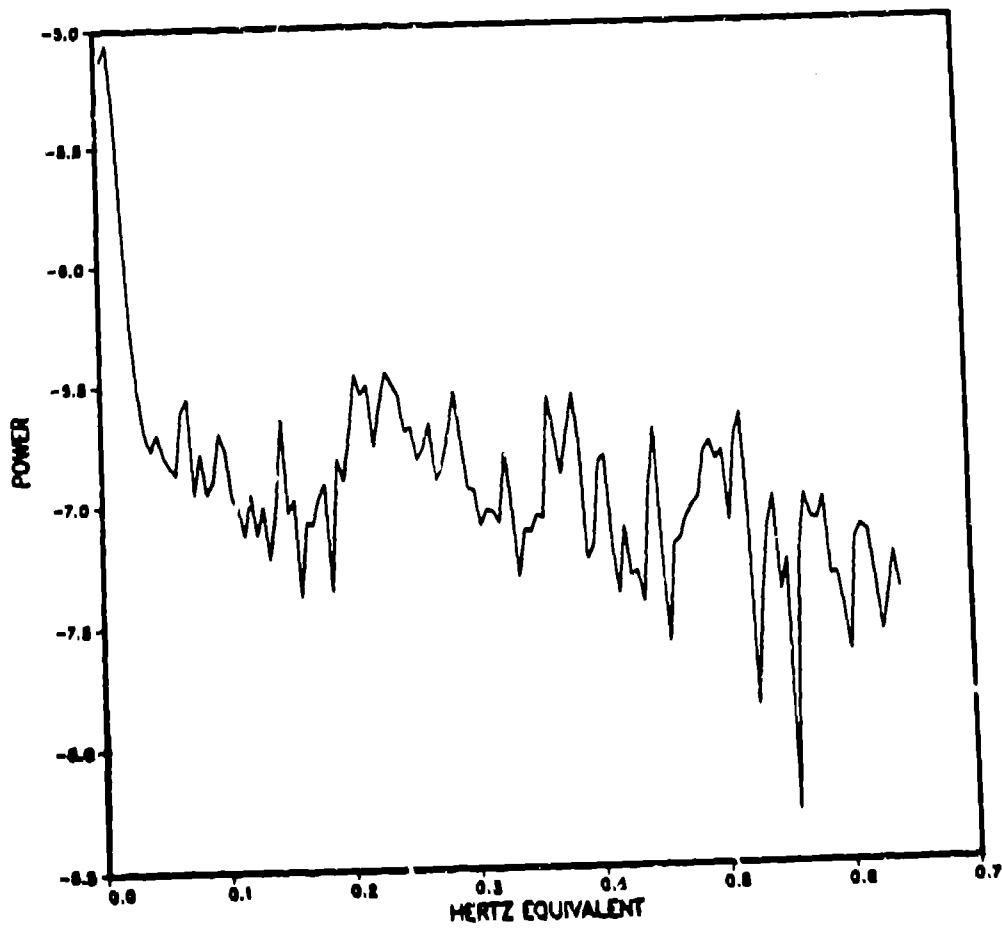
1271



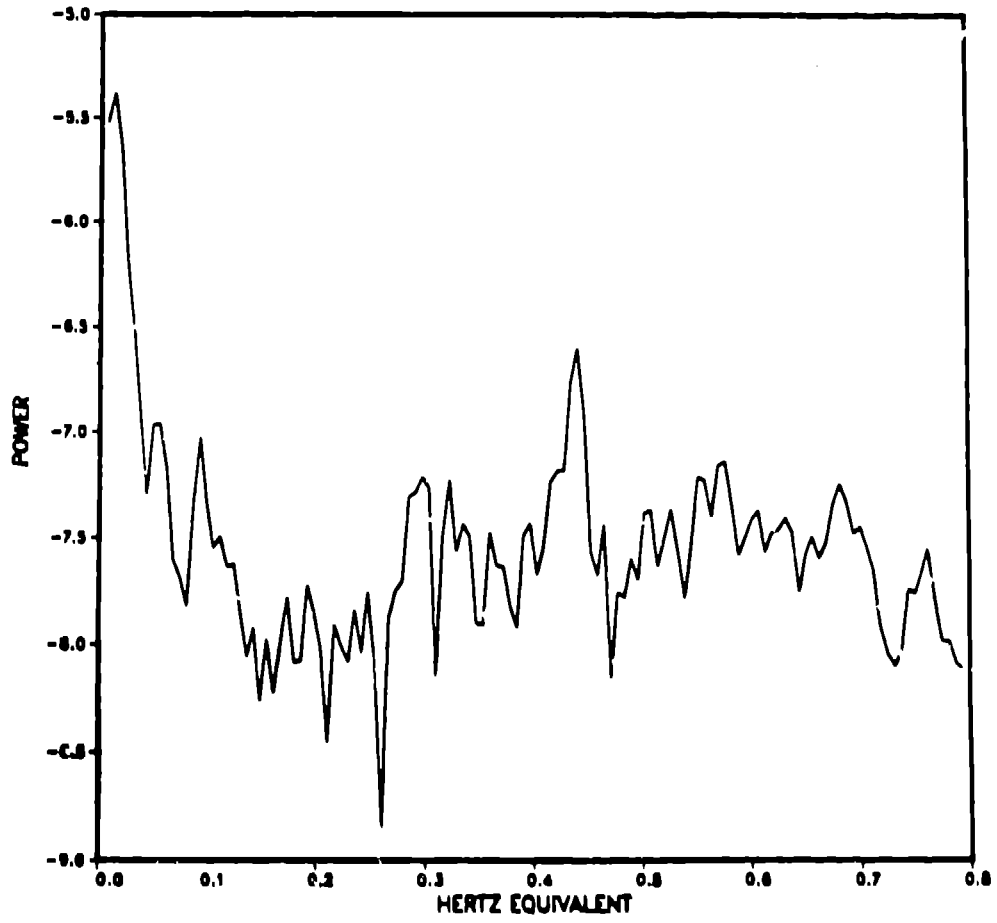
16M



8212

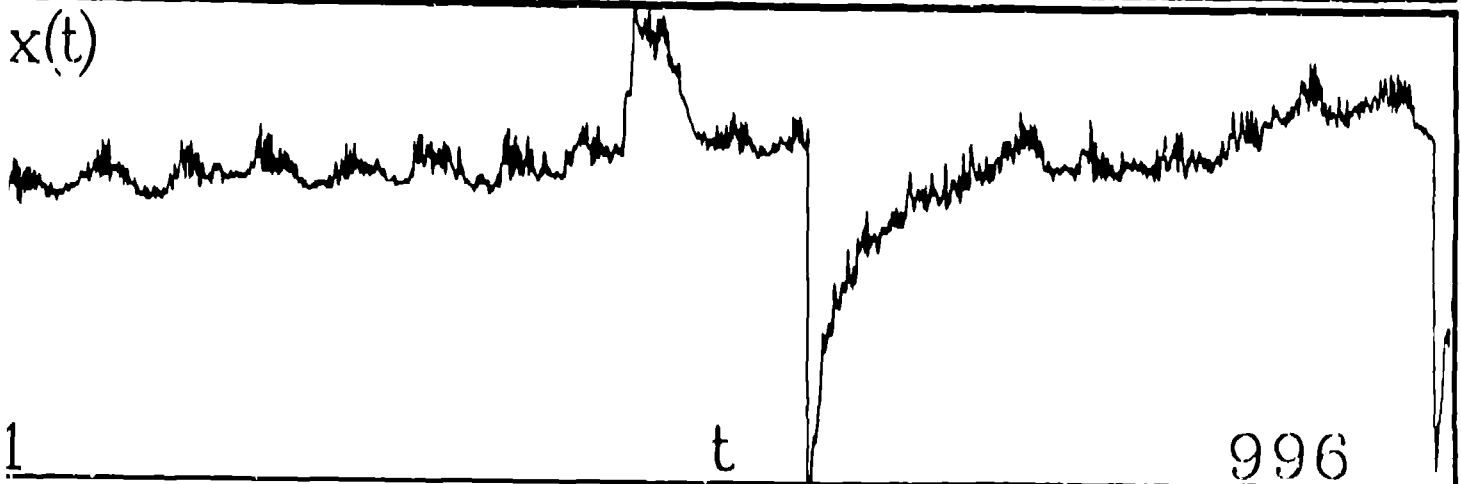
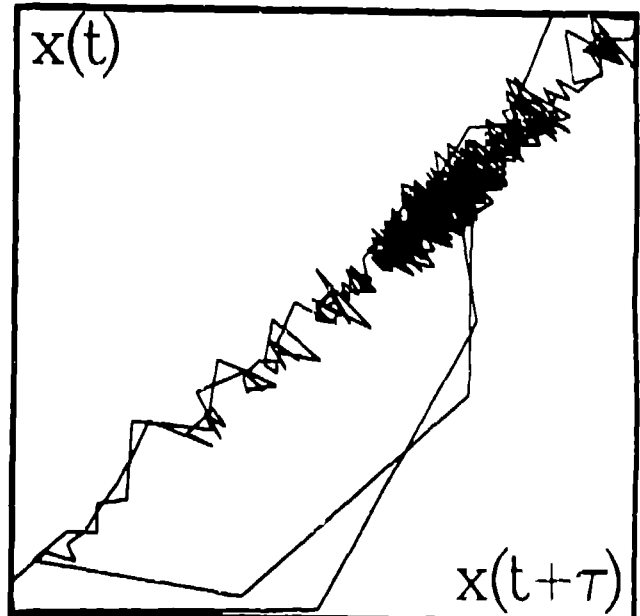
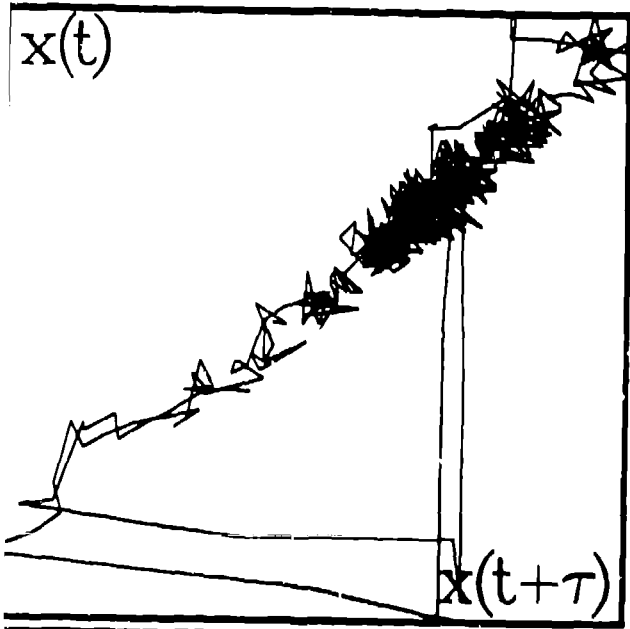


1726



$\tau_2 = 4$ run 1271

$\tau_1 = 1$



run 1611

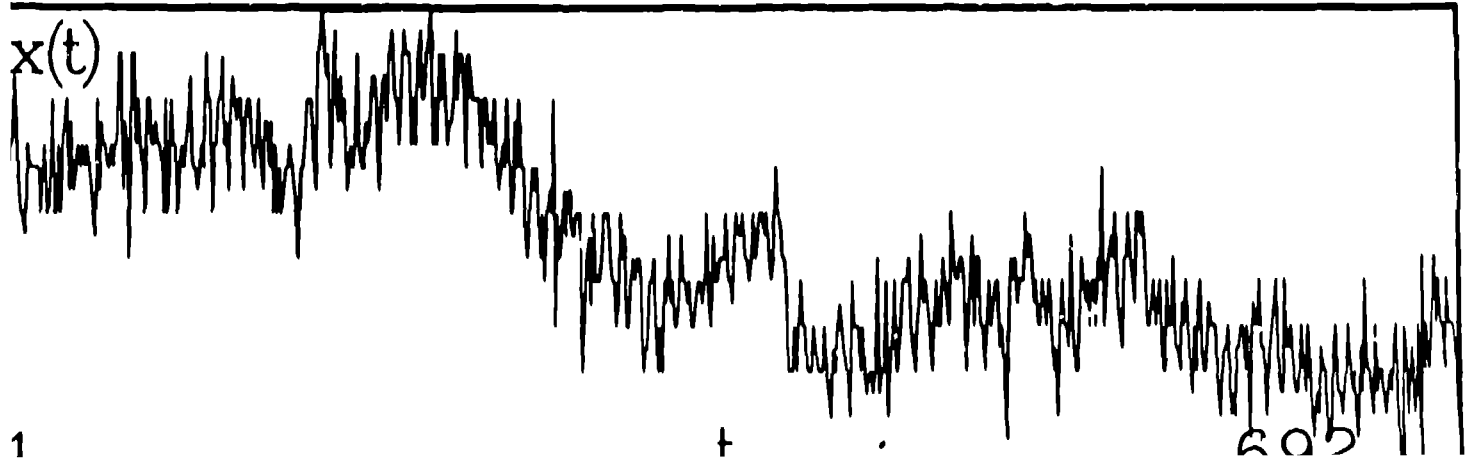
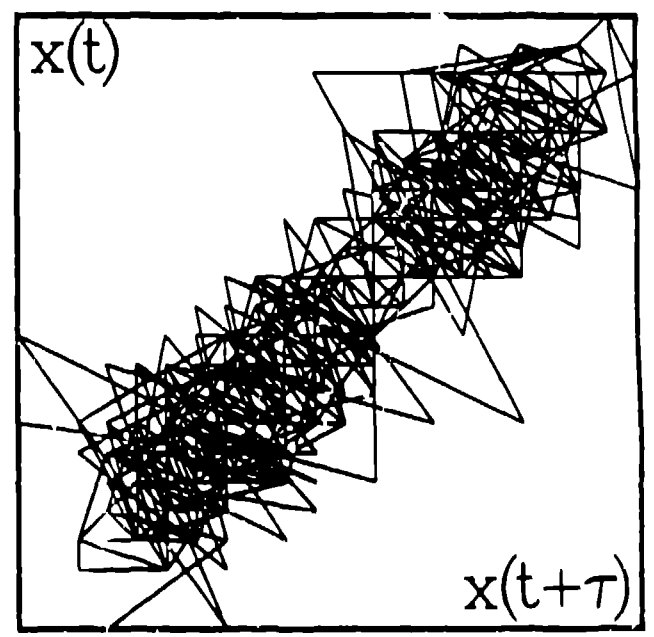
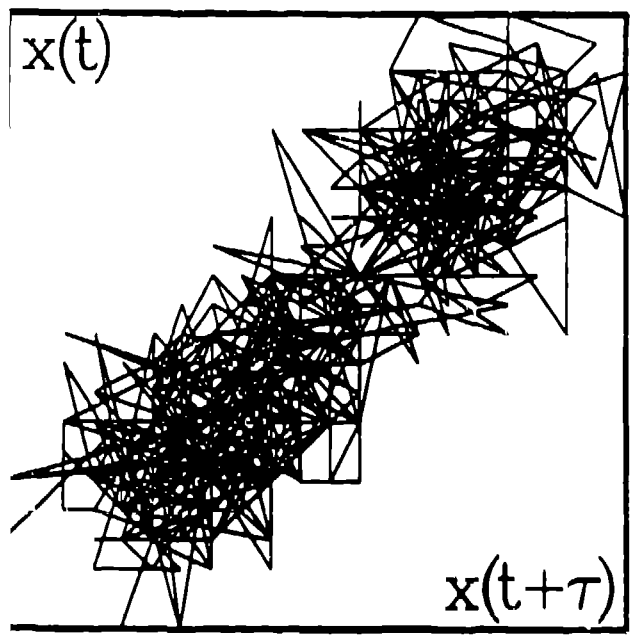
41 712

Fig 7

$\tau_2 = 4$

run 1611

$\tau_1 = 1$



1

t

205

~~ku~~ ~~1379~~

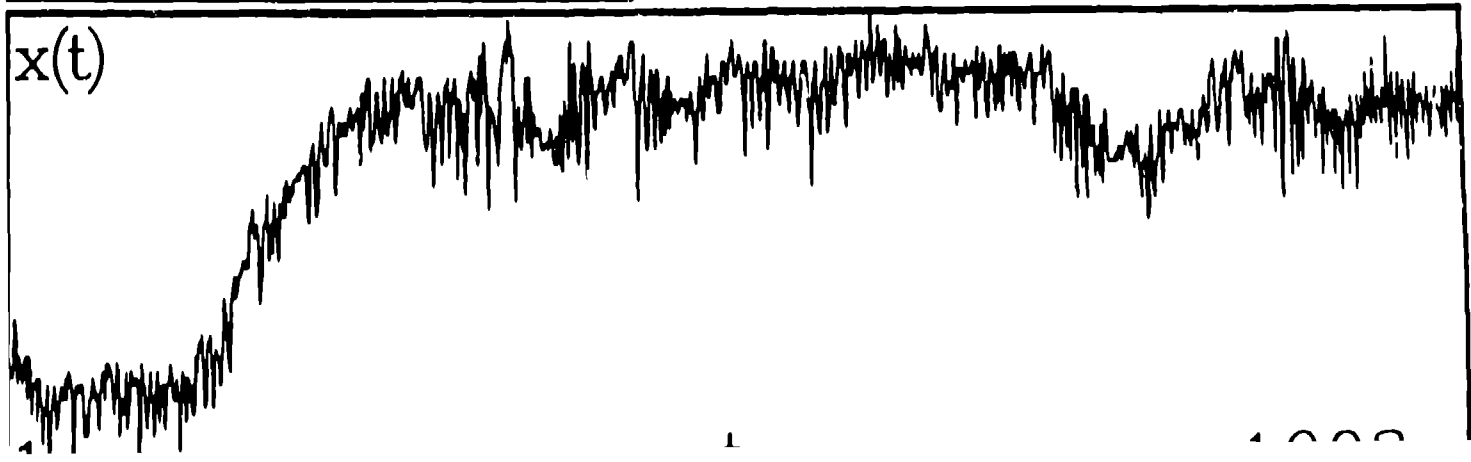
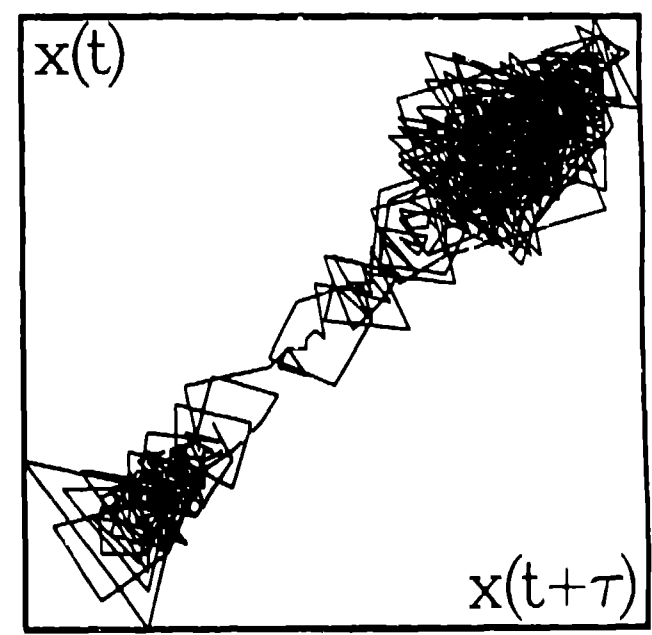
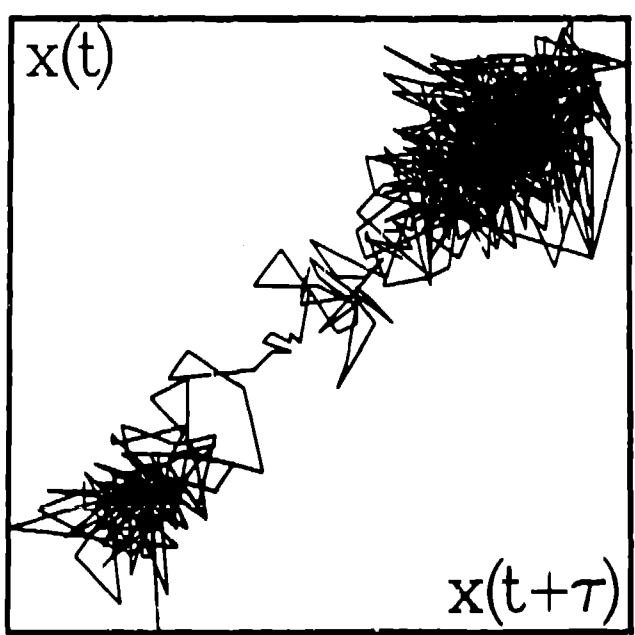
~~000~~

0.1

1/28

$\tau_2 = 4$

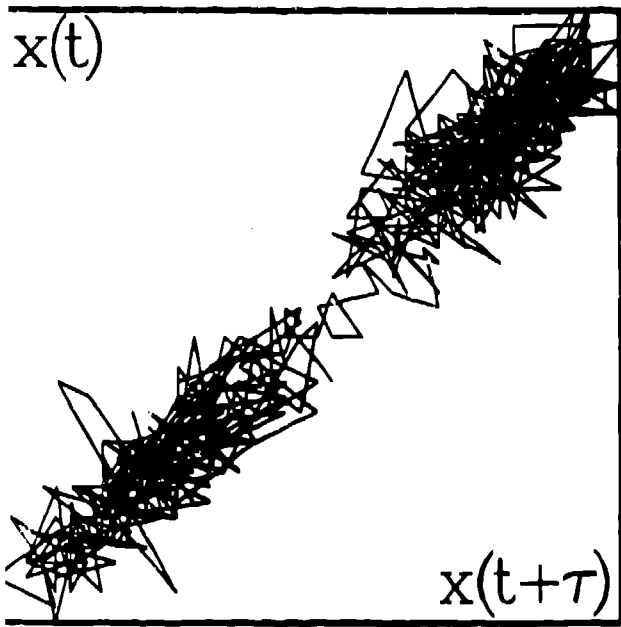
$\tau_1 = 1$



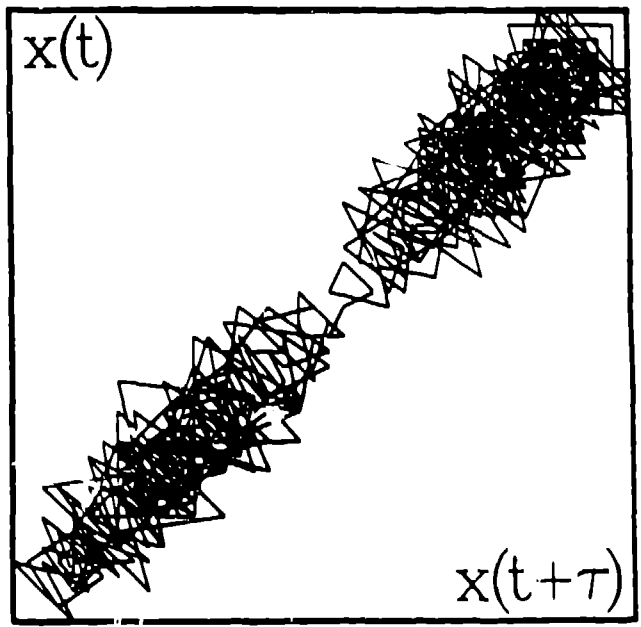
Ex 101 16

Fig 1

$$\tau_2 = 4$$



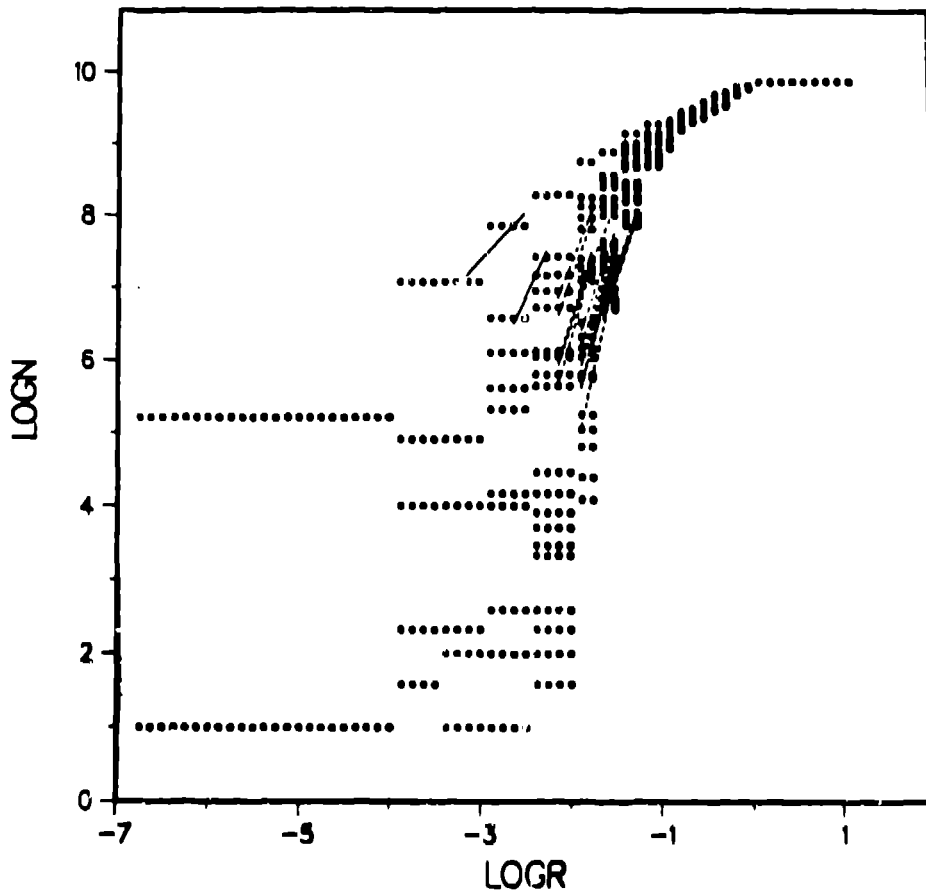
$$\tau_1 = 1$$



1.FILE: SP1611O KREF:100

NSEC : 1	NDTOT : 1024	NDAT : 939
NREF : 200	KREF : 100	FTGUE: 0.20
IRNU1 : 4	NDELAY: 4	NWIND : 4

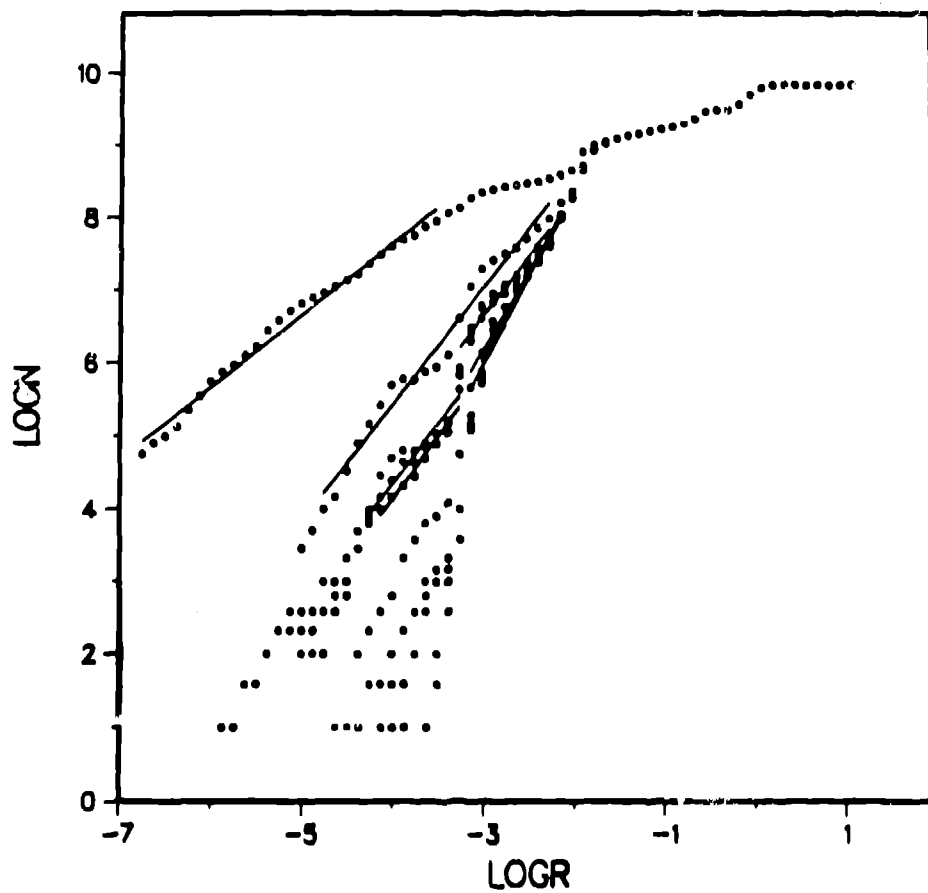
NO SING. VALUE DECOMPOSITION



1.FILE: SP1611B KREF:100

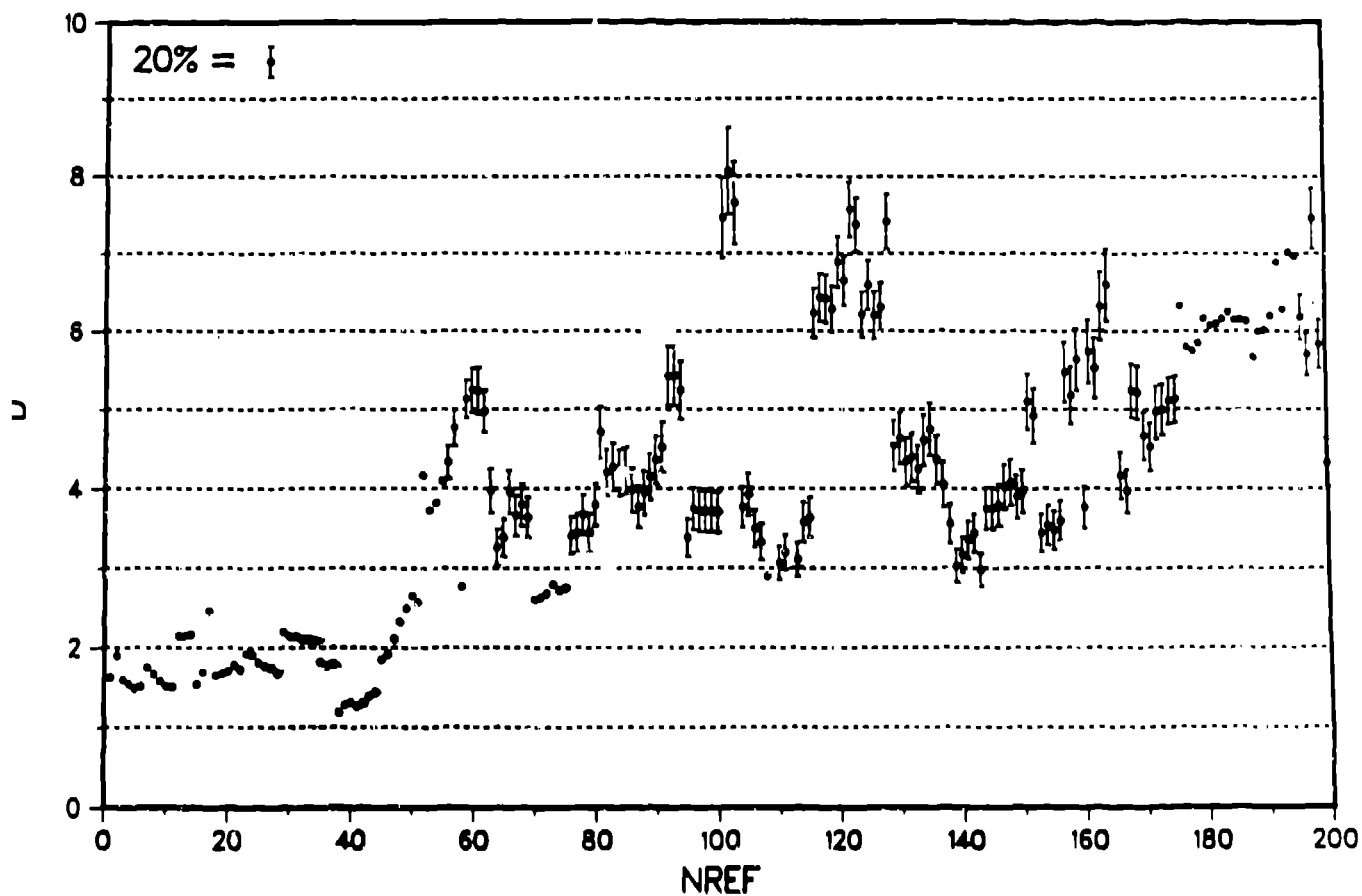
NSEG : 1	NDTOT : 1024	NDAT : 916
NREF : 200	KREF : 100	FIGUE: 0.20
IRNU1 : 4	NDELAY: 1	NWIND : 4

SING .VALUE DECOMP. BY COV. MATRIX



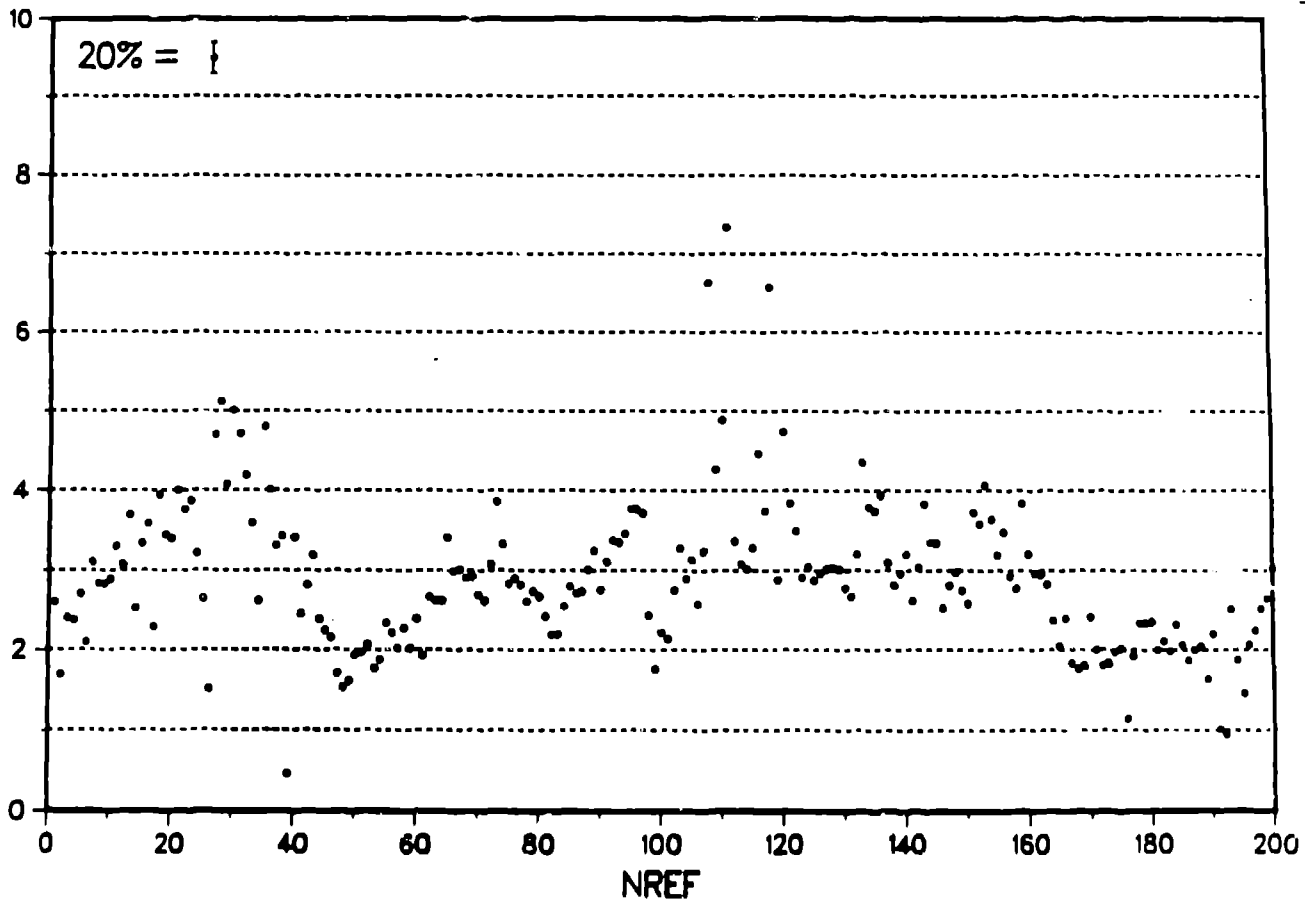
1.FILE: SF16110 NDIM:20

NSEG : 1 NDTG NDAT : 939
NREF : 200 KREF FTIGUE: 0.20
IRNU1 : 4 NDELA NWIND : 4
NREFOK :83
NO SING. VALUE DECOMPOSITION



1.FILE: SP1611B NDIM:20

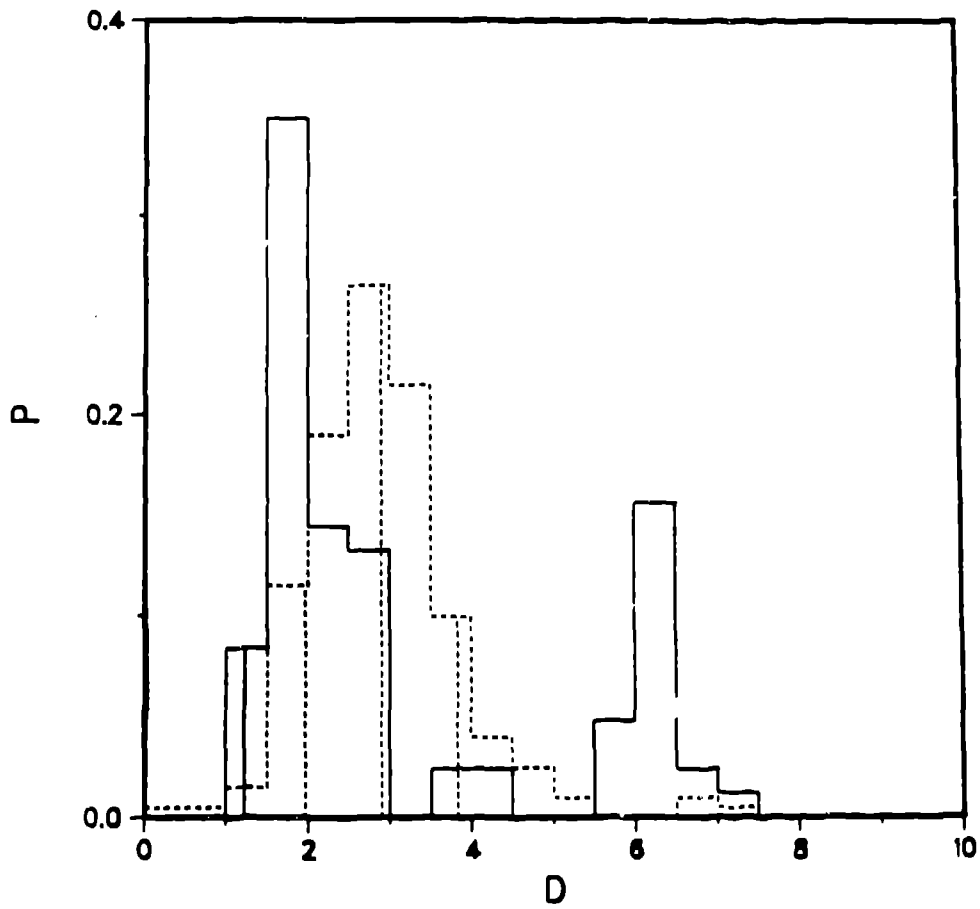
NSEG : 1 NDTOT : 1024 NDAT : 916
NREF : 200 KREF : 100 FITGUE: 0.20
IRNU1 : 4 NDELAY: 1 NWIND : 4
NREFOK :200
SING .VALUE DECOMP. BY COV. MATRIX



2.FILE: ~~SRI151BR1511020~~DIM:20

NSEG : 1	NDTOT : 1024	NDAT : 939
NREF : 200	KREF : 100	FTGUE: 0.20
IRNU1 : 4	NDELAY: 4	NWIND : 4
NREFOK :83	DIM20: 3.08	STA20: 1.86

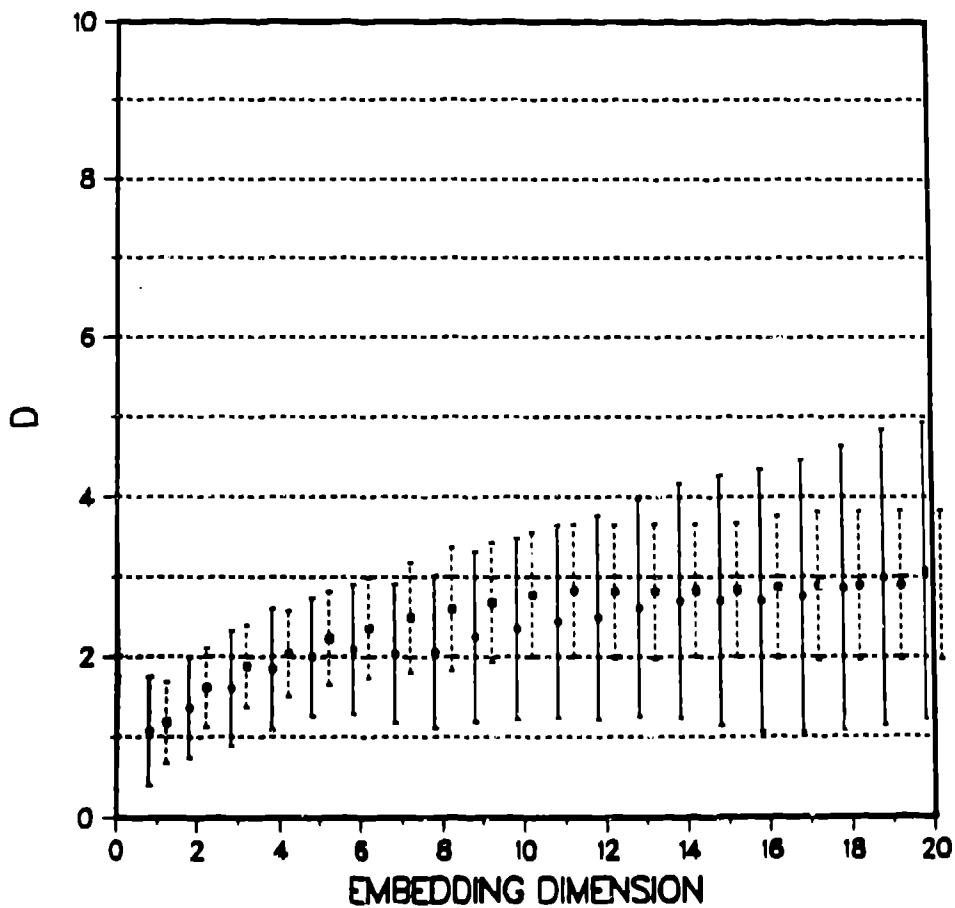
NO SING. VALUE DECOMPOSITION



2.FILE: ~~SP16110~~ SP16110

NSEG : 1	NDTOT : 1024	NDAT : 939
NREF : 200	KREF : 100	FTGUE: 0.20
IRNU1 : 4	NDELAY: 4	NWIND : 4
NREFOK : 83	DIM20: 3.08	STA20: 1.86

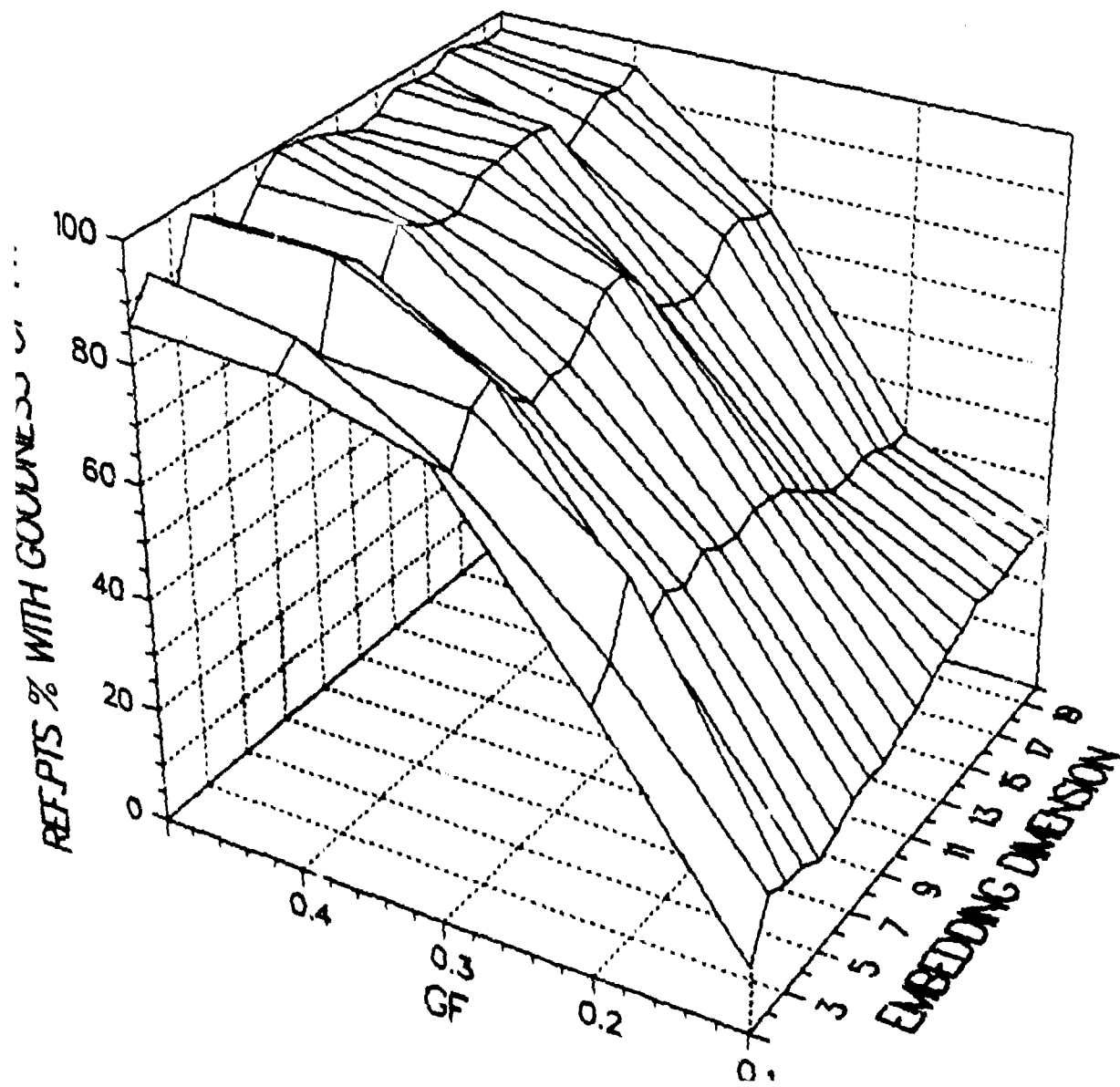
NO SING. VALUE DECOMPOSITION



1.FILE: SP16110

NSEG : 1	NDTOT : 1024	NDAT : 939
NREF : 200	KREF : 100	FITGUE: 0.20
IRNU1 : 4	NDELAY: 4	NWIND : 4

NO SING. VALUE DECOMPOSITION

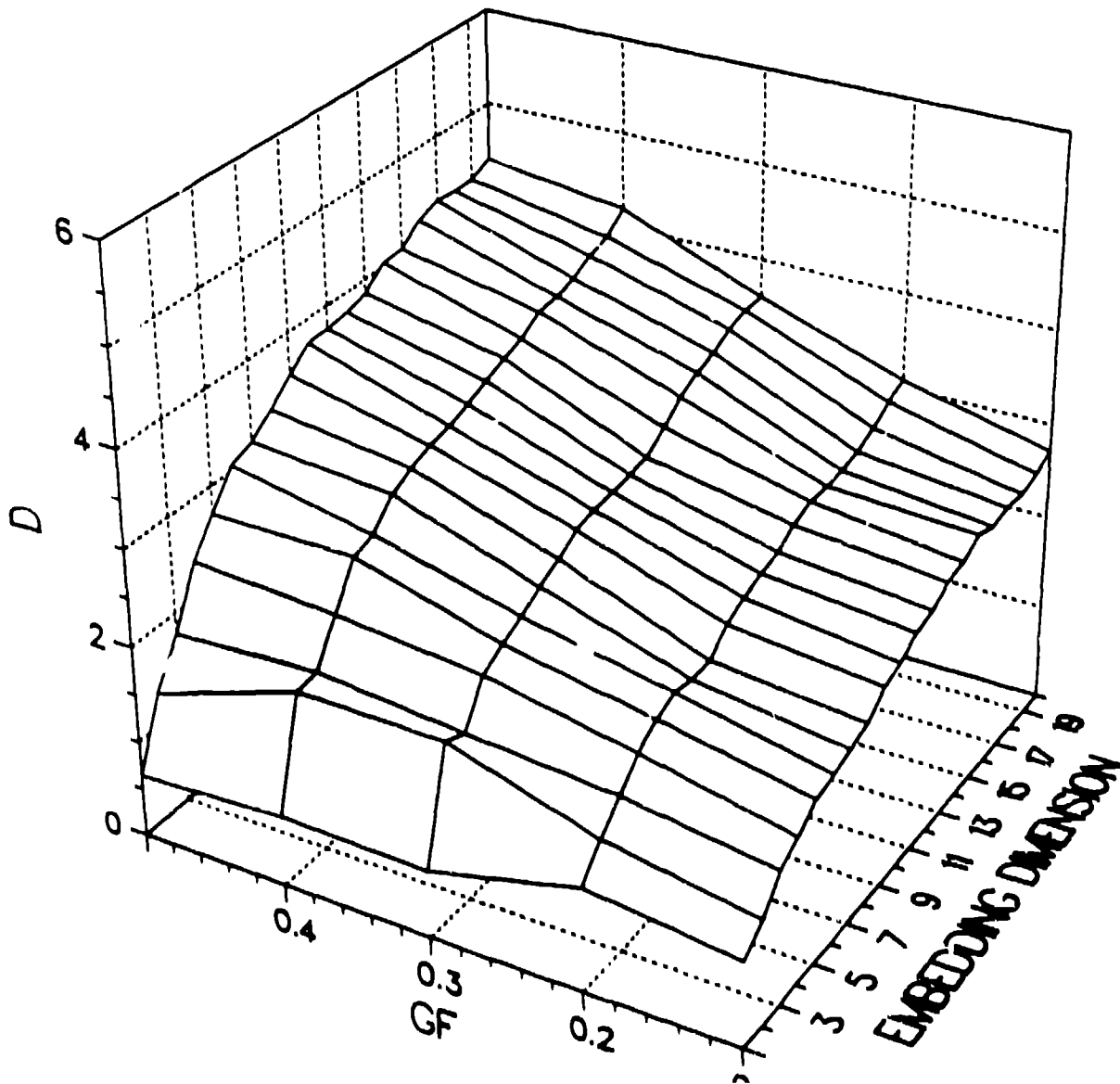


1-0-14

T:FILE: SP16110

NSEG : 1	NDTOT : 1024	NDAT : 939
NREF : 200	KREF : 100	FITGUE: 0.20
IRNU1 : 4	NDELAY: 4	NWIND : 4

NO SING. VALUE DECOMPOSITION

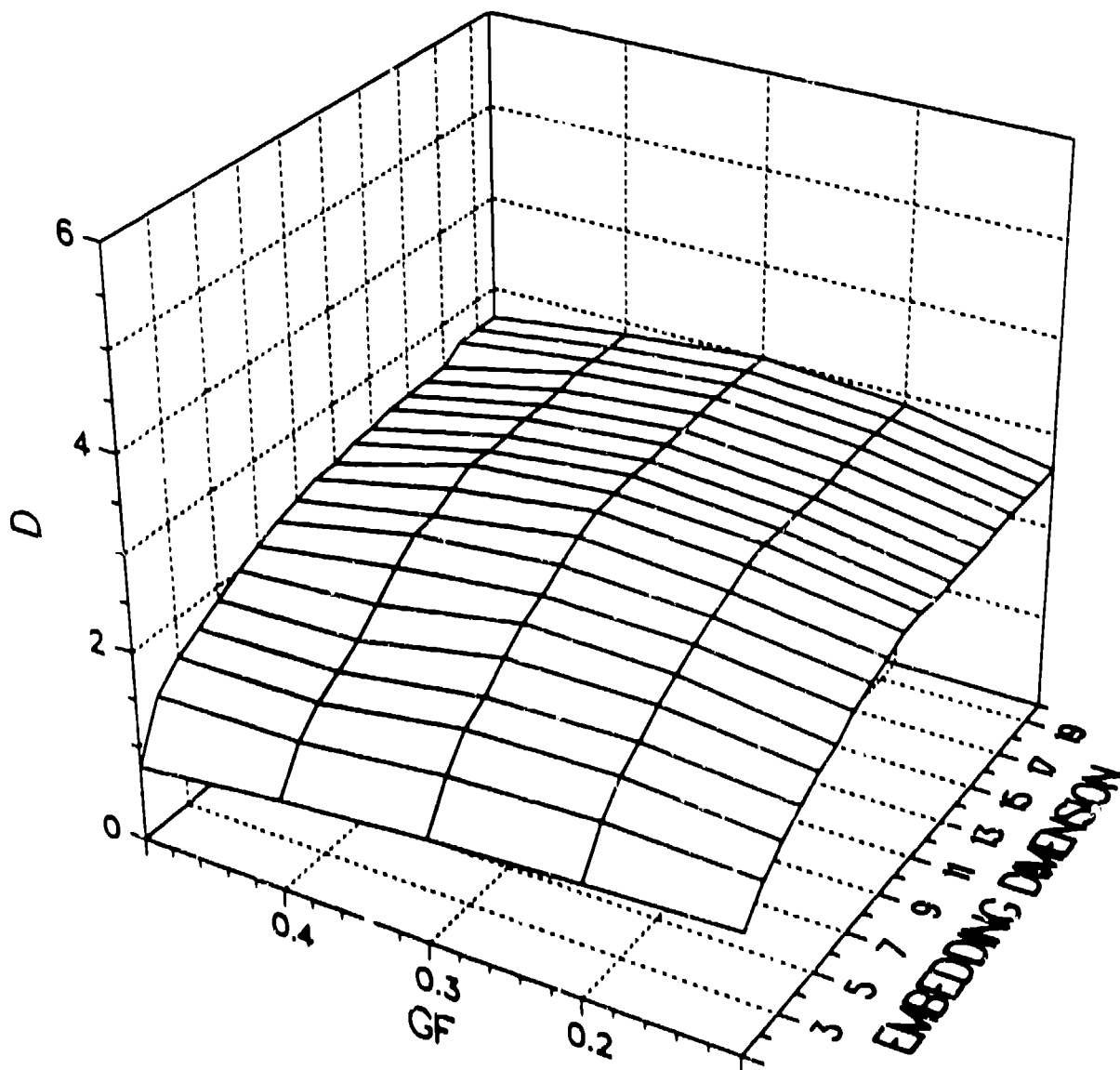


02/13

1.FILE: SP1611B

NSEG : 1	NDTOT : 1024	NDAT : 916
NREF : 200	KREF : 100	FITGUE: 0.20
IRNU1 : 4	NDELAY: 1	NWIND : 4

SING .VALUE DECOMP. BY COV. MATRIX

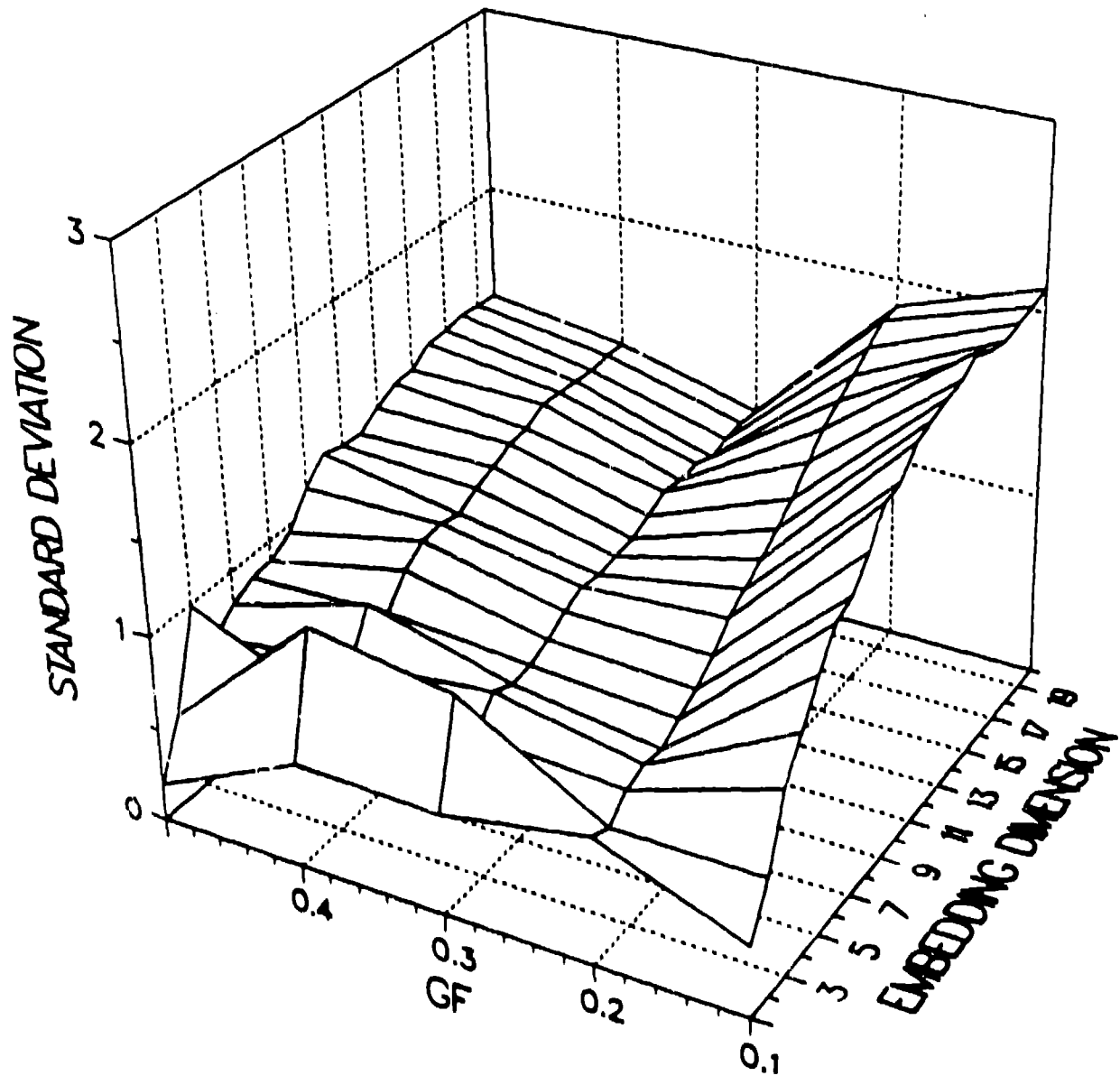


1.13

1.FILE: SP16110

NSEG : 1	NDTOT : 1024	NDAT : 939
NREF : 200	KREF : 100	FTGUE: 0.50
IRNU1 : 4	NDELAY: 4	NWIND : 4

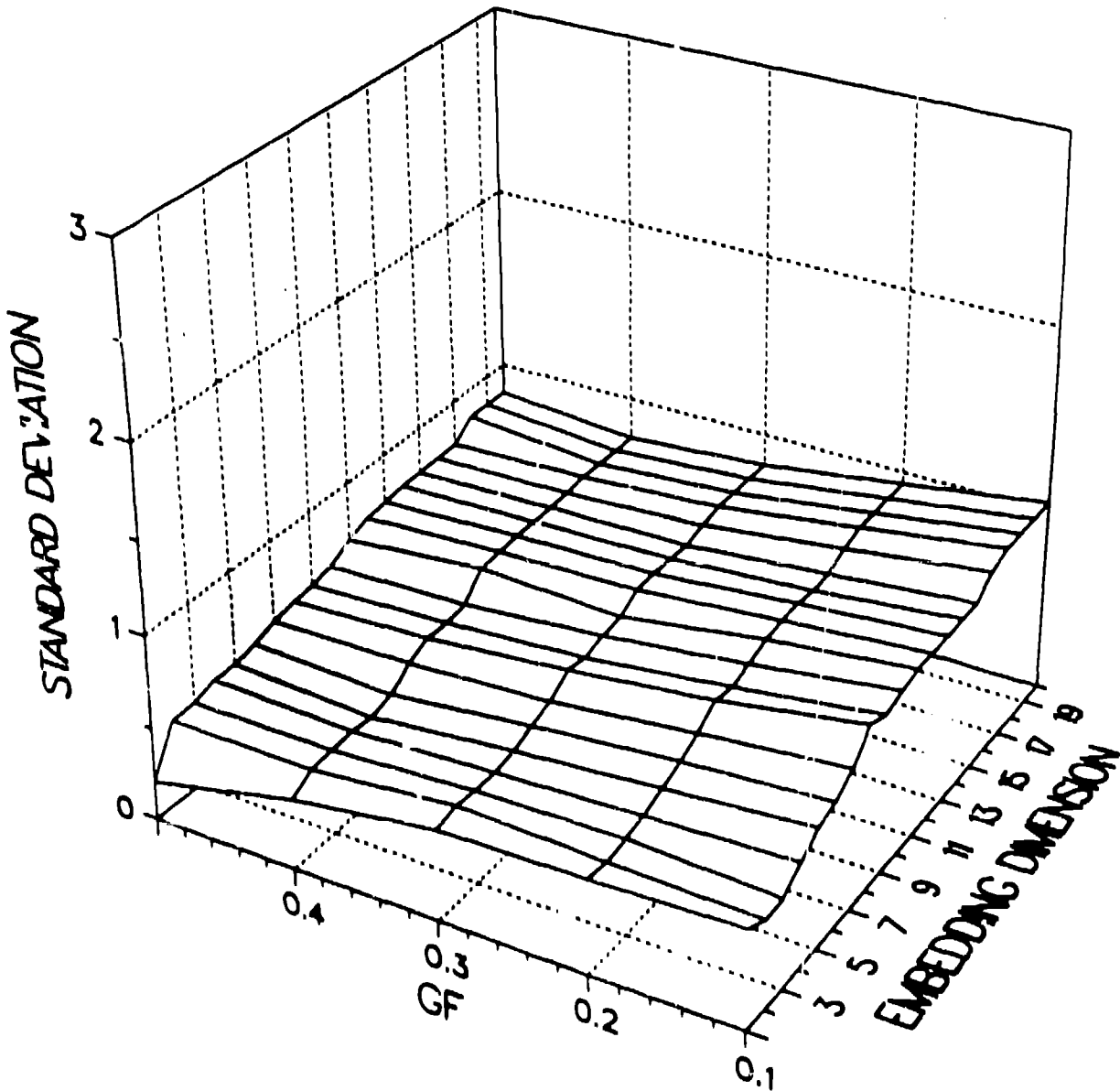
NO SING. VALUE DECOMPOSITION



T.FILE: SP1611B

NSEG : 1	NDTOT : 1024	NDAT : 916
NREF : 200	KREF : 100	FITGUE: 0.50
IRNU1 : 4	NDELAY: 1	NWIND : 4

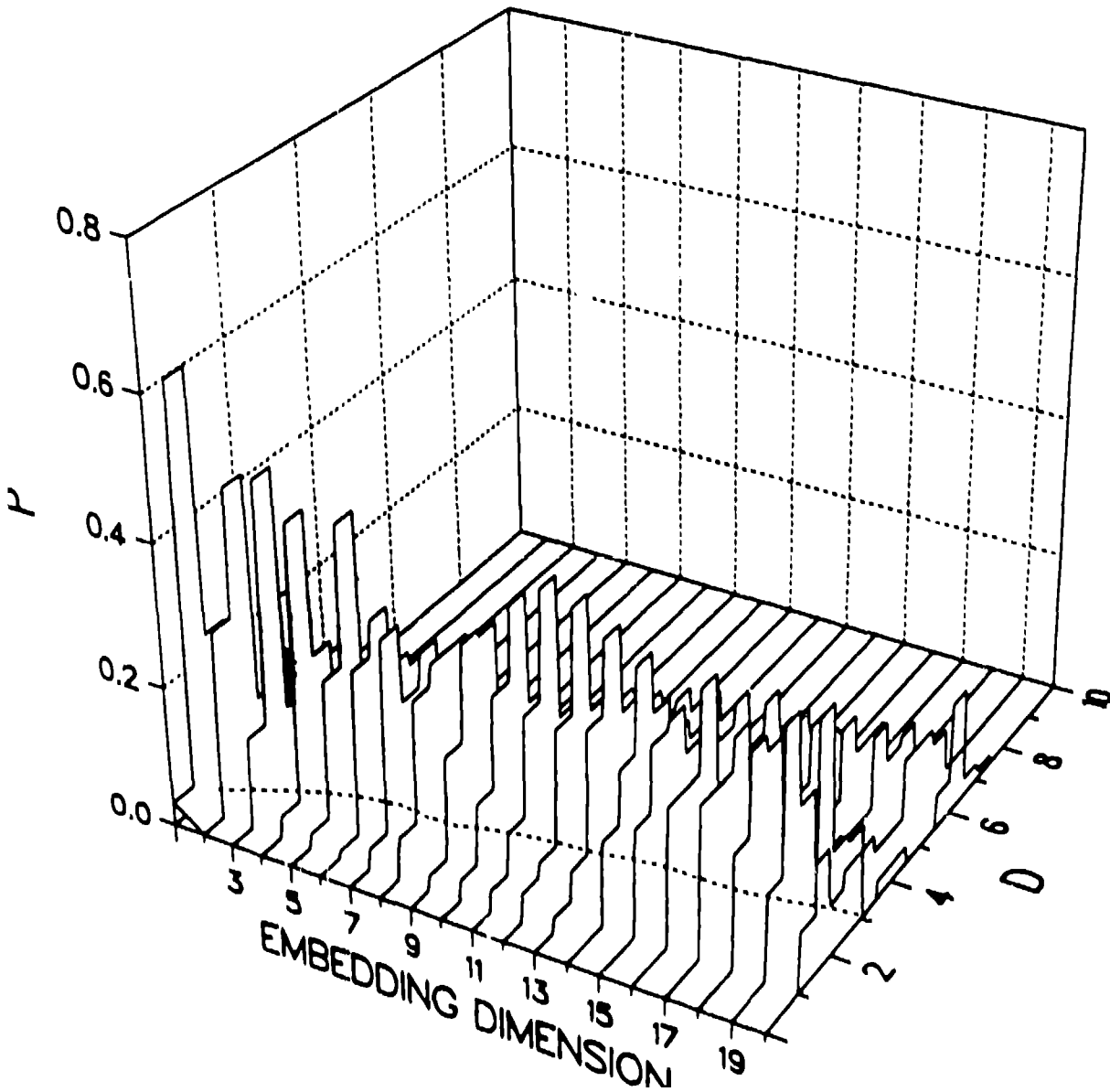
SING .VALUE DECOMP. BY COV. MATRIX



1. FILE: SP16110

NSEG : 1 NDTOT : 1024 NDAT : 939
NREF : 200 KREF : 100 FITGUE: 0.50 0.2
IRNU1 : 4 NDELAY: 4 NWIND : 4

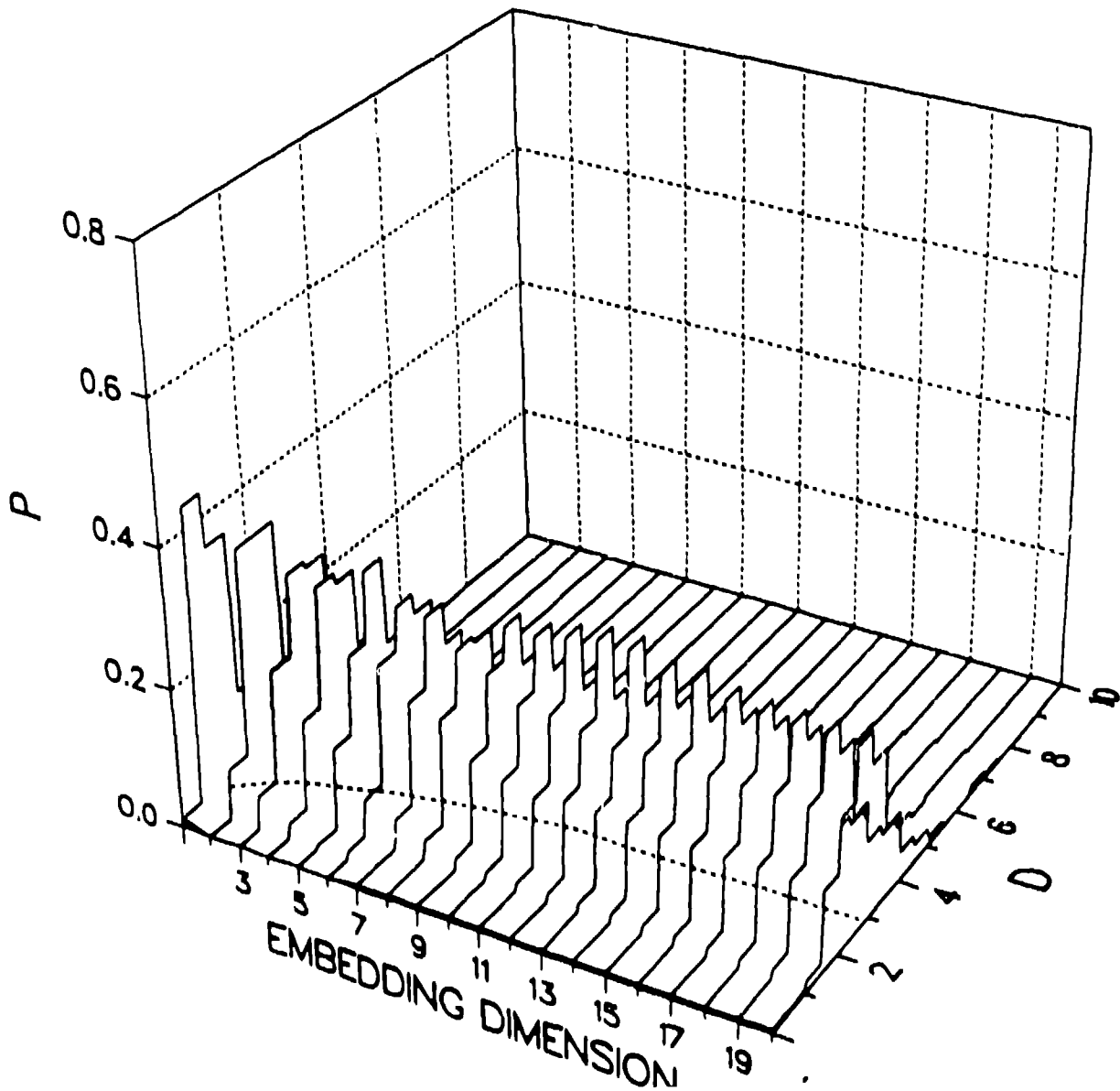
NO SING. VALUE DECOMPOSITION



T.FILE: SP1611B

NSEG : 1 NDTOT : 1024 NDAT : 916
NREF : 200 KREF : 100 FITGUE: ~~0.50~~ 0.2
IRNU1 : 4 NDELAY: 1 NWIND : 4

SING .VALUE DECOMP. BY COV. MATRIX

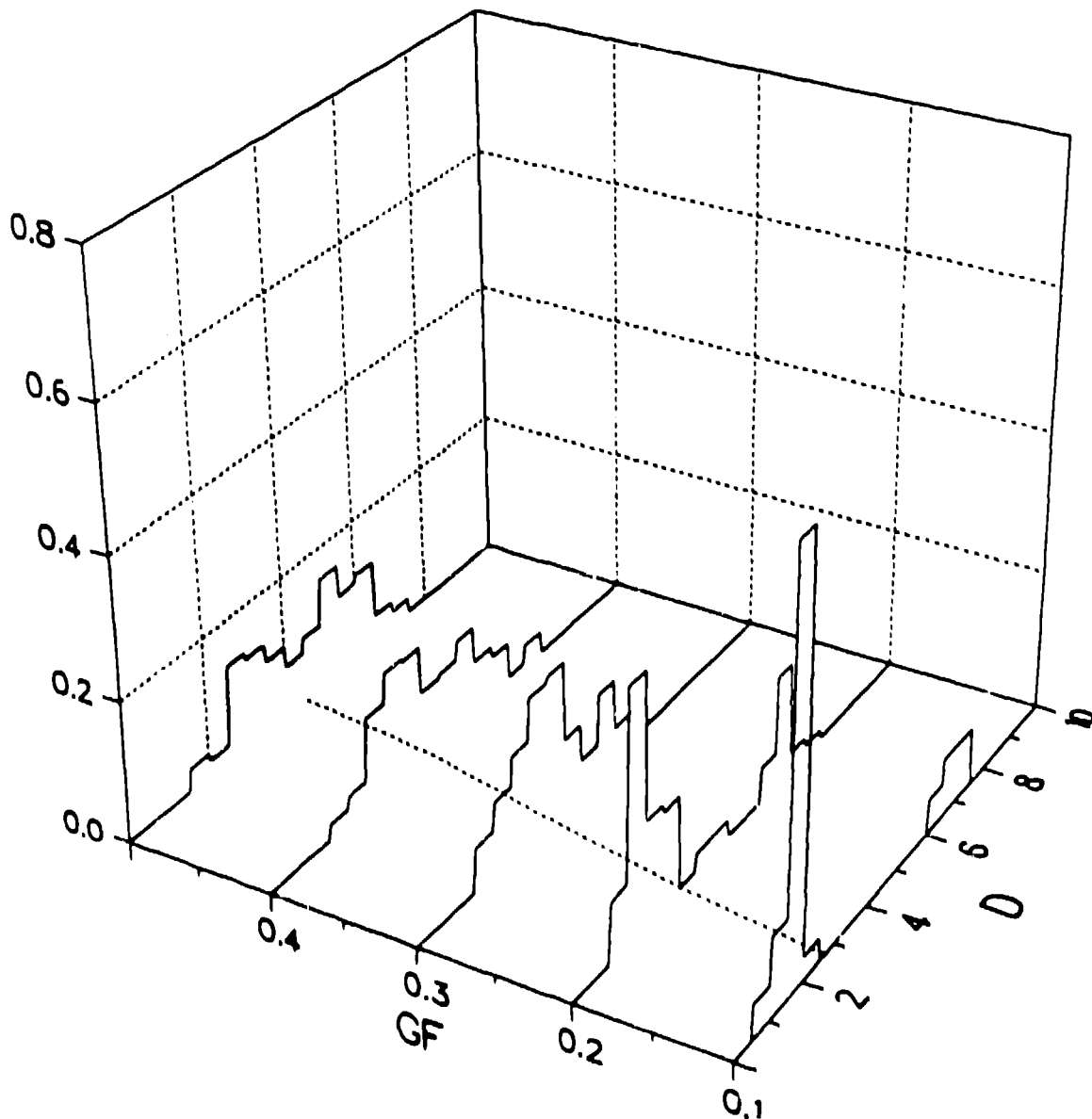


5375

1.FILE: SP16110 NDIM:20

NSEG : 1	NDTOT : 1024	NDAT : 939
NREF : 200	KREF : 100	FITGUE: 0.20
IRNU1 : 4	NDELAY: 4	NWIND : 4

NO SING. VALUE DECOMPOSITION

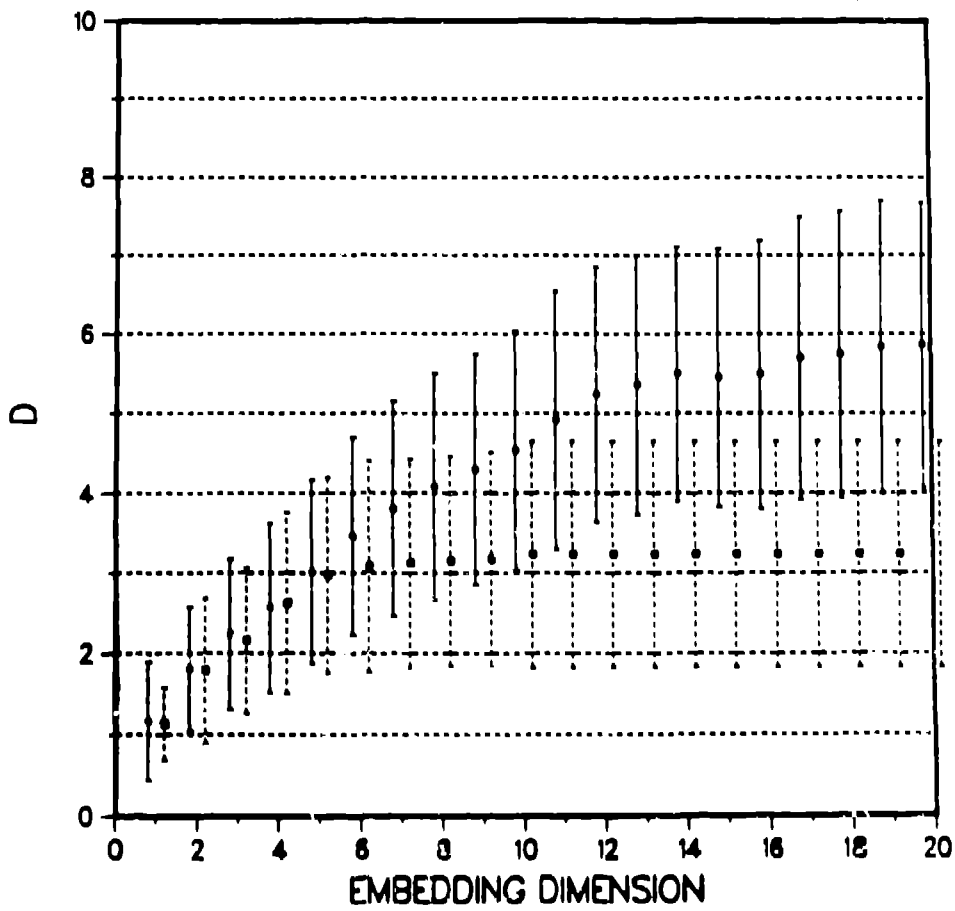


1.20-1

ds

2.FILE: ~~SRI127~~ SP12710

NSEG : 1 NDTOT : 1024 NDAT : 939
NREF : 200 KREF : 100 FITGUE: 0.20
IRNU1 : 4 NDELAY: 4 NWIND : 4
NREFOK : 172 DIM20: 5.87 STA20: 1.80
NO SING. VALUE DECOMPOSITION



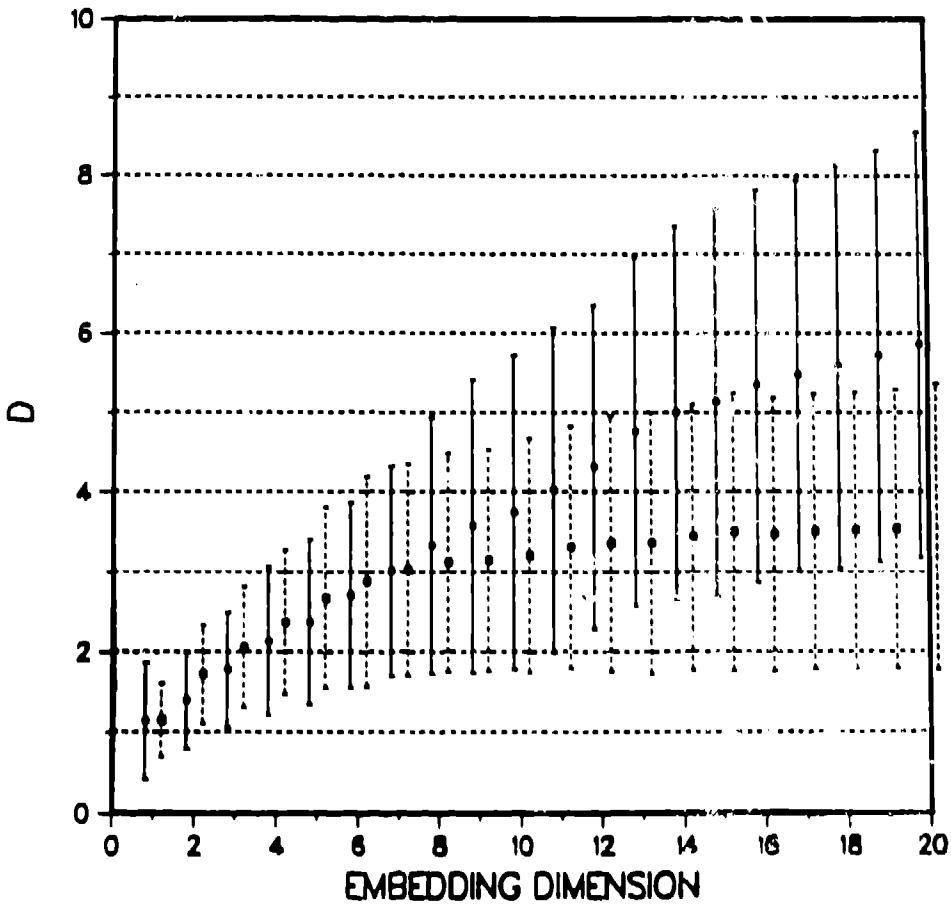
ref

2.1.1

Li

2.FILE: ~~SRR~~21882120

NSEG : 1 NDTOT : 1024 NDAT : 939
NREF : 200 KREF : 100 FITGUE: 0.20
IRNU1 : 4 NDELAY: 4 NWIND : 4
NREFOK :168 DIM20: 5.86 STA20: 2.69
NO SING. VALUE DECOMPOSITION



clcc

2.FILE: ~~SM1726~~BT7260

NSEG : 1	NDTOT : 1024	NDAT : 939
NREF : 200	KREF : 100	FTGUE: 0.20
IRNU1 : 4	NDELAY: 4	NWIND : 4
NREFOK :101	DIM20: 3.54	STA20: 1.63

NO SING. VALUE DECOMPOSITION

